UNIVERSITY OF MALTA

Faculty of Science

Department of Geosciences

DISSERTATION

M.Sc. in Applied Oceanography

Innovative Methods for Detecting Sea Turtle Nests: A Combination of UAV Photogrammetry, GPR, and Artificial Intelligence for Non-Invasive Monitoring and Conservation

by

Barbora Fürychová

Supervised by Dr. Emanuele Colica

A dissertation submitted in partial fulfilment of the requirements of the award of Master of Science in Applied Oceanography of the University of Malta

Acknowledgements

I would like to express my sincere gratitude to everyone who contributed to this research and supported me throughout my work on this thesis.

First and foremost, I would like to thank my supervisor, Dr. Emanuele Colica, for his valuable guidance, insightful suggestions, and continuous support during my research.
My thanks also go to Prof. Sebastiano D'Amico for his input during the early stages of this project.
My special thanks are extended to Dr. Adam Gauci for his exceptional help with data processing and coding.

Finally, I am deeply grateful to my family for always standing by me and providing endless encouragement and understanding throughout this journey.

Abstract

Sea turtle nesting represents one of the most vulnerable stages in their life cycle; therefore, protecting nesting sites is essential for the long-term survival of their populations. Traditional nest detection methods are often invasive and may disturb nesting females. This study introduces a non-invasive approach for detecting and monitoring sea turtle nests through the combined use of advanced technologies. Specifically, Ground Penetrating Radar (GPR) and Artificial Intelligence (AI) are employed to automatically identify turtle tracks and assist in locating potential nesting sites.

As part of this study, fieldwork was conducted at Golden Bay, Malta, where a simulated nest of loggerhead turtle (*Caretta caretta*) was put together to evaluate how effectively and accurately GPR can find an underground chamber containing eggs. To confirm the radar data, a 3D LiDAR model was made of the internal structure of the simulated nest, thus providing a reference dataset for the interpretation of radargrams. Meanwhile, an AI algorithm was instructed to automatically recognize turtle tracks from beach photos, thus facilitating the identification of potential nesting areas.

The integrative approach of these techniques demonstrates the potential of non-invasive technologies to enhance the efficiency of sea turtle nest detection and conservation. The findings contribute to the development of modern conservation strategies, particularly within small Mediterranean rookeries such as Malta, where nesting events are rare and spatially constrained.

Contents

List of Figures

List of Tables

List of Acronyms

3D	Three-Dimensional
AI	Artificial Intelligence
CNN	Convolutional Neural Network
CMS	Convention on the Conservation of Migratory Species of Wild Animals
CITES	Convention on International Trade in Endangered Species of Wild Fauna and Flora
CR	Critically Endangered
DFL	Distribution Focal Loss
EN	Endangered
ERA	Environment and Resources Authority (Malta)
ETD	Electronic Theses and Dissertations
GFCM	General Fisheries Commission for the Mediterranean
GPR	Ground Penetrating Radar
ICCAT	International Commission for the Conservation of Atlantic Tunas
IUCN	International Union for Conservation of Nature
IoU	Intersection over Union
LiDAR	Light Detection and Ranging
MSFD	Marine Strategy Framework Directive
PCB(s)	Polychlorinated Biphenyl(s)
SfM	Structure from Motion

POPs	Persistent Organic Pollutants
TED	Turtle Excluder Device
UAV	Unmanned Aerial Vehicle
UNEP	United Nations Environment Programme
VU	Vulnerable
YOLO	You Only Look Once (object detection algorithm)
WWF	World Wide Fund for Nature

Aim and Objectives

The primary aim of this study is to develop and test a combination of non-invasive techniques for detecting sea turtle nests, ensuring accurate and efficient conservation efforts while minimizing disturbance to their natural environment.

To achieve this, the research focuses on several key objectives. Ground Penetrating Radar (GPR) is assessed for its efficiency in detecting buried sea turtle nests, with initial validation conducted using chicken eggs in a controlled experiment.

Additionally, AI-based track recognition is developed by training a machine learning model to identify sea turtle track patterns from aerial images.

To enhance data visualization and spatial interpretation, a mobile-based photogrammetric approach enhanced by LiDAR depth sensing was employed to create a 3D model of a simulated sea turtle nest. This method enabled precise visualization of the nest's internal structure and supported accurate spatial analysis.

The study further integrates these techniques to evaluate their combined effectiveness and feasibility for large-scale, non-invasive monitoring of sea turtle nesting areas.

1. Introduction

Sea turtles represent one of the oldest groups of marine vertebrates, with evolutionary lineages that can be traced back more than 100 million years (Bowen & Karl, 2007). Although they have survived dramatic climatic and geological changes, their populations have experienced a sharp decline in recent centuries due to human activities (Spotila, 2004). The most vulnerable stage of their life cycle is the nesting period, during which the females come ashore from the sea and thus become exposed to a number of terrestrial risks - ranging from being preyed upon to suffering from light pollution. Consequently, the reproductive success of sea turtles is highly dependent on the condition of the coastal ecosystems (Eckert, 1999).

Out of the seven species of sea turtles that have survived, only the loggerhead turtle (*Caretta caretta*) and the green turtle *(Chelonia mydas*) are nesting in the Mediterranean Sea.

The nesting areas of *C. mydas* are mostly limited to the eastern Mediterranean whereas *C. caretta* in the last years has relocated its nesting grounds to the central part of the Mediterranean including Malta, where it is the only species that nests regularly within the archipelago (Vella & Vella, 2023).

The Mediterranean Sea serves as an important regional reproductive and migratory area for the loggerhead turtle. Most nesting sites can be found mainly in Greece, Turkey, Libya, and Cyprus, while Malta is situated at the central part of the migratory corridor (Casale & Margaritoulis, 2010). The establishment of nests in Malta is thus indicative of a local population expansion or recovery of the regional population (Casale & Margaritoulis, 2010).

Sea turtles are essential in keeping marine ecosystems healthy. One example is Green turtles (*Chelonia mydas*), which influence the dynamics of seagrass meadows by feeding, thus the regeneration and the growth of new shoots are promoted, and over time the productivity and biodiversity of these habitats are enhanced (Bouchard & Bjorndal, 2000). On the other hand, the population of Hawksbill turtles (*Eretmochelys imbricata*) on coral reefs is involved in the regulation of sponge species, thus they contribute to the maintenance of the ecological balance of coral reefs (Spotila, 2004). Through these ecological interactions, sea turtles contribute to the

stability and functionality of marine habitats, and their decline can lead to significant disruption of ecosystem balance.

Another important ecological function of sea turtles is the transfer of nutrients between the marine and terrestrial environments. Eggshells, unhatched eggs, and dead hatchlings enrich sandy dunes with organic material, thereby enhancing organic matter and supporting the growth of vegetation that helps stabilize the coastline (Bouchard & Bjorndal, 2000). Sea turtles are therefore considered keystone species, whose decline can trigger cascading changes throughout the ecosystem (Spotila, 2004).

Historically, sea turtles have been part of human culture and economy for millennia. However, main hunting of the animals for meat, oil, and turtle shell during the 19th and 20th centuries was the reason why the population of sea turtles dropped dramatically (Hays, 2005; Spotila, 2004). Presently, to mention a few, trade in turtle products is prohibited under CITES and the Bern Convention. Despite these restrictions, the harvesting of nests for the purpose of trade and the killing of female adults for meat is still happening in several parts of the world (Troëng et al., 2007).

According to the International Union for Conservation of Nature (IUCN), most sea turtle species are either endangered or critically endangered. The main causes of their population decline include the loss of nesting habitats due to coastal development, direct hunting, bycatch in fisheries, marine pollution, and climate change (Lewison et al., 2004; Hawkes et al., 2007). Rising sand temperatures during incubation lead to a higher proportion of females, which may, in the long term, destabilize population balance (Hawkes et al., 2007). Traditional nesting monitoring methods mostly require digging the sand which can lead to eggs being harmed or changing their microclimatic conditions (Eckert, 1999). These risks highlight the urgent need for modern, non-invasive nest monitoring solutions that cause no harm to the natural surroundings while fulfilling monitoring requirements.

Despite these threats, there are examples of successful conservation. Long-term monitoring program in Tortuguero, Costa Rica, has been able to prove that continuous nest safeguarding and control of human intervention on natural habitats can bring the return of population - the number of green turtle (*Chelonia mydas*) nesting females has elevated by over 400% since the 1970s

(Troëng et al., 2007; Dutton et al., 2005). These findings underline the significance of long-term research and evidence-based conservation management.

Conservation of sea turtles is thus interlinked with the health of not only these individuals but the whole coastal and marine ecosystems. The development of non-invasive technologies that enable the monitoring and protection of turtle nests without disturbing their natural conditions represents a crucial step towards the sustainable conservation of these key marine organisms (Vella & Vella, 2023). This thesis therefore focuses on the combination of non-invasive techniques that provide more accurate and less invasive detection of sea turtle nests.

2. Literature Review

2.1 Biology and Life Cycle of Sea Turtles

Sea turtles represent one of the most ancient lineages of marine vertebrates, with fossil evidence indicating their evolutionary origins extend back over 100 million years (Bowen & Karl, 2007). Though they have changed to diverse oceanic ecosystems over time, they all have several morphological and behavioral traits common to them. A characteristic example is certainly their hard or leather-like carapace which provides protection against predators while simultaneously reducing drag during swimming (Spotila, 2004).

Adult sea turtles are predominantly herbivorous, particularly species such as the green turtle (*Chelonia mydas*) which can be seen on Figure 1. However, the juveniles of most species exhibit carnivorous feeding behavior, gradually shifting to a plant-based diet as they mature. Their life cycle is highly adapted to marine conditions, yet reproduction takes place on land, where females come ashore to lay their eggs on sandy beaches. This return to their birthplace, known as philopatry, is one of the most remarkable phenomena in the animal kingdom (Lee et al., 2007).

Females typically lay between 80-120 eggs in a chamber dug in the sand with their hind flippers, where the eggs are covered and left to incubate for approximately 50-70 days (Ackerman, 1997). Both the length of the incubation period and the sex ratio of hatchlings depend on the temperature of the sand: the warmer the sand is, the more females hatch, while lower temperatures result in a higher number of males (Mrosovsky et al., 1984; Hawkes et al., 2007).

After hatching, the hatchlings instinctively orient themselves towards the sea, guided by light and temperature gradients (Lohmann et al., 1990). This phase, known as the *swim frenzy*, represents a period of intense activity during which hatchlings attempt to reach the open ocean and escape predators (Hays, 2005). The probability of survival at this stage is extremely low – it is estimated that only one out of a thousand hatchlings will eventually reach sexual maturity (Robinson & Paladino, 2013). The following *oceanic stage* is spent in the pelagic environment, where juveniles remain for several years, often seeking refuge among floating Sargassum algae. Upon reaching a

certain size, they enter the *neritic stage*, becoming more benthic and inhabiting coastal areas rich in food resources (B., 2002).

Sea turtles mature sexually very late, usually between 20 and 40 years of age (Spotila, 2004). Such a slow life cycle together with high juvenile mortality rates makes sea turtles highly vulnerable to environmental changes and anthropogenic pressures. Females return to nest roughly every 2-4 years, and during a single nesting season, they can have multiple clutches (Hirth, 1971).

Figure 1. Green sea turtle (Chelonia mydas). Photos by Henry Copperstone (2025).

Although all seven species of sea turtles share similar reproductive cycles and ecological requirements, they differ in size, dietary specialization, and geographic distribution (Spotila, 2004). These variations reflect their adaptations to various marine environments ranging from tropical coral reefs to colder oceanic areas. Table 1 summarizes the fundamental ecological characteristics of each species.

Table 1. Overview of the seven species of sea turtles and their main characteristics (Spotila, 2004; Hirth, 1971; IUCN Red List, 2024).

Species	**Scientific Name**	**Family**	**Type of Carapace**	**Main Diet**	**Distribution**	**IUCN Status**
Green turtle	*Chelonia mydas*	Cheloniidae	hard	seagrasses, algae	tropical and subtropical regions	Endangered (EN)
Hawksbill turtle	*Eretmochelys imbricata*	Cheloniidae	hard	marine sponges	tropical coral reef regions	Critically Endangered (CR)
Loggerhead turtle	*Caretta caretta*	Cheloniidae	hard	crustaceans, molluscs	Atlantic, Indian, and Mediterranean oceans	Vulnerable (VU)
Kemp's ridley turtle	*Lepidochelys kempii*	Cheloniidae	hard	crustaceans	western Atlantic, Gulf of Mexico	Critically Endangered (CR)
Olive ridley turtle	*Lepidochelys olivacea*	Cheloniidae	tvrdý	molluscs, fish	tropical oceans	Endangered (EN)
Leatherback turtle	*Dermochelys coriacea*	Dermochelyidae	leathery	jellyfish	tropical and temperate oceans	Vulnerable (VU)
Flatback turtle	*Natator depressus*	Cheloniidae	hard	benthic fauna	northern Australia	Endangered (EN)

2.2 Nesting Behavior and Reproduction

Nesting represents the most vulnerable stage in the life cycle of sea turtles, when females leave the safety of the marine environment and expose themselves to terrestrial risks (Spotila, 2004). This process is only possible on beaches covered with sand, whose physical features such as grain size, temperature, moisture, and slope highly determine the success of nests (Ackerman, 1997; Hirth, 1997). The female tortoises look for safe, silent, and dark places on the shore that have not been visited or disturbed by anyone to lay their eggs there (Spotila, 2004).

After emerging from the sea, the female begins by excavating a shallow body pit with her front flippers. Once this is nearly complete, she uses her hind flippers to deepen and widen the hole, forming the chamber of the nest. At a certain depth which is usually around 30-60 cm and also varies according to the species and the sand characteristics egg laying begins (Ackerman, 1997). Oviposition occurs in short intervals, with eggs deposited in several small batches until the chamber is filled.

The eggs of sea turtles are enclosed in a soft, leathery shell, which is very permeable, thus it allows the gases to pass through the shell and hence the embryo can develop even if there is only a limited supply of oxygen in the surrounding environment. The embryo's development is sustained by a system of extraembryonic membranes that collectively provide protection, nourishment, and gas exchange. The amnion is a membrane that contains fluid which serves as a cushion for the embryo and also the fluid helps in keeping stability, on the other hand, the yolk sac is the main source of nutrients. The allantois is responsible for the gas exchange and also it removes the metabolic waste, whereas the chorion binds the whole system to the outside through the pores in the eggshell (Spotila, 2004). The structure of the egg is shown in Figure 2.

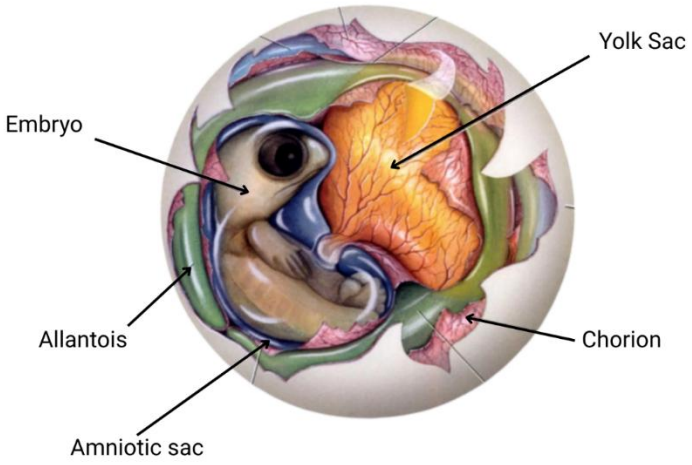

Figure 2. Structure of a sea turtle egg showing the embryo and its associated extraembryonic membranes, the amnion, yolk sac, chorion, and allantois, which together ensure protection, nutrition, and gas exchange during embryonic development (adapted from Spotila, 2004).

After laying her eggs, the female covers the chamber with moist sand and then spreads a layer of dry sand over it to hide the precise location of the nest. This behavior reduces the risk of predation and protects the clutch from temperature extremes. After camouflaging the place, the female returns to the sea and never revisits the nest. The eggs and hatchlings are thus left entirely to natural environmental factors (Spotila, 2004).

The number of eggs in a clutch varies according to the species and the body size of the female. On average, a clutch contains between 80 and 120; however, the flatback turtle (*Natator depressus*) has only about 50 eggs, while the hawksbill turtle (*Eretmochelys imbricata*) can lay more than 200 eggs (WWF, 2000). Females may lay between two and eight clutches per season, and most species do not nest annually but at intervals of two to four years (Hirth, 1997). Incubation lasts approximately 50 to 70 days. If a female is disturbed during oviposition, she may abandon the process and return to the sea, a phenomenon known as a false crawl, which represents an unsuccessful nesting attempt (Spotila, 2004).

When the incubation period ends, the hatchlings begin to break out of their eggs and gradually move upward through the sand. They usually emerge during the night, when lower temperatures and reduced activity on the beach minimize the risk of predation. Upon reaching the surface, they instinctively orient themselves toward the sea (Spotila, 2004).

The journey from the nest to the sea is extremely energy-demanding, hatchlings may lose up to 20% of their body weight due to dehydration and physical exhaustion (Spotila, 2004). Predation during this stage is intense, with threats from crabs, birds, mammals, and marine fish. Once hatchlings reach the sea, ocean currents carry them into open water, where their oceanic developmental phase begins. Males never return to land after reaching maturity, while females return to their natal beaches after two to three decades to repeat the nesting cycle (Ackerman, 1997).

2.3 Threats and Risk Factors

Sea turtles are currently facing from a variety of anthropogenic threats that are interrelated and have a major impact on their survival. The most serious factors include incidental capture in fisheries (bycatch), loss and degradation of nesting habitats, pollution of the ocean, and climate change. These factors act synergistically, jointly reducing reproductive success and the ability of populations to recover (Lewison et al., 2004; Casale & Margaritoulis, 2010).

Bycatch, the inadvertent capture of turtles in fishing nets, on longlines, or in other fishing gear, is one of the leading causes of sea turtle deaths. In such cases, the animal usually dies from suffocation as it is unable to release itself and get back to the water surface to breathe (Lewison et al., 2004). In the Mediterranean Sea, where the loggerhead turtle (*Caretta caretta*) is the most common, bycatch accounts for the most significant source of mortality among the adult individuals (Alessandro & Antonello, 2010).

To reduce this risk, various technical modifications have been developed, such as Turtle Excluder Devices (TEDs), which allow turtles to escape from trawl nets (Figure 3.). In addition, international initiatives have been established within organisations such as the International Commission for the Conservation of Atlantic Tunas (ICCAT) and the General Fisheries Commission for the Mediterranean (GFCM), with the aim of minimising unwanted bycatch (GFCM, n.d.; ICCAT, n.d.; Vella & Vella, 2023).

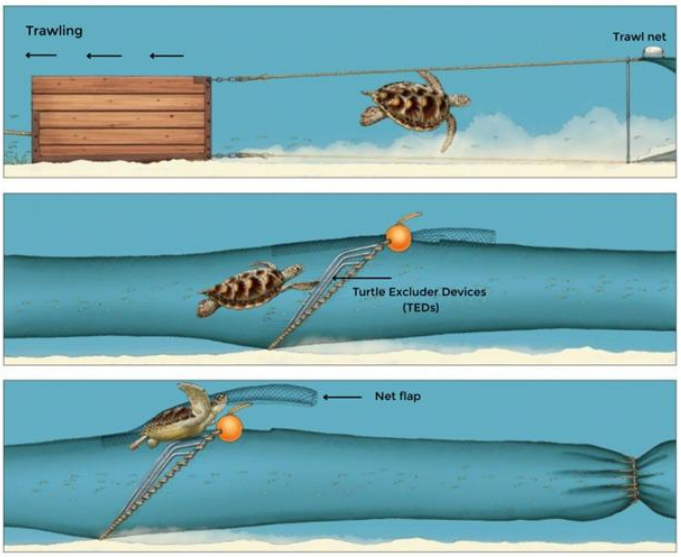

Figure 3. Illustration of the functioning of Turtle Excluder Devices (TEDs) installed in trawl nets, allowing sea turtles to escape while retaining target catch (adapted from Pilcher, 2014).

Another major threat is the loss of nesting habitats is the disappearance of nesting habitats because of destruction of the coast, tourism, and erosion. Artificial lighting also causes disorientation of hatchlings, which often move toward inland light sources instead of the sea, leading to high mortality rates (Witherington et al., 2011). Besides, artificial light confuses the hatchlings, which frequently head for the light coming from the land instead of the sea, thus resulting in high death rates (Bolten & Witherington, 2003). This issue has also been recorded in Malta, where cases of unsuccessful nesting have been observed due to excessive sand moisture or compaction following storms (Vella & Vella, 2023).

Figure 4. Sea turtle with a severely fractured carapace caused by a boat collision. (Source: Nature Trust Malta, 2024).

Marine pollution is another serious problem that the world is facing, and it is a significant factor in the decrease of marine fauna. Sea turtles commonly mistaken plastic bags and sheets for jellyfish, which can result in intestinal blockage, cessation of digestion, and death. Plastic debris is now present in all components of the marine ecosystem and affects a wide spectrum of organisms, from plankton to large vertebrates. Sea turtles are particularly vulnerable because of their migratory behavior and use of diverse habitats, including nesting beaches. The consumption of plastics may cause internal injuries, lower food intake, and may lead to starvation, reflected in decreased growth, reproductive success, and overall health condition. Microplastics pose a chronic risk as they can accumulate in tissues and disrupt hormonal and immune functions, while also exerting indirect effects through food web alterations and changes in the physical properties of nesting beaches (Nelms et al., 2016).

Figure 5. Dead sea turtle entangled in discarded fishing gear collected by Nature Trust Malta. (Source: Nature Trust Malta, 2024).

The contamination of marine environments with heavy metals, pesticides, and persistent organic pollutants (POPs), such as polychlorinated biphenyls (PCBs), represents another significant stressor for sea turtles. The study by Storelli & Marcotrigiano (2003) documented high concentrations of mercury, cadmium, and lead in the liver, kidneys, and muscles of sea turtles, indicating long-term bioaccumulation of these substances within the food chain. These contaminants can disrupt metabolism, cause damage to hepatic and renal tissues, and pose a potential risk to embryonic development, as metals can be transferred to the eggs. Chronic exposure to heavy metals and organic pollutants can therefore lead to decreased vitality of adult individuals and reduced reproductive success (Storelli & Marcotrigiano, 2003).

Climate change affects all stages of the sea turtle life cycle. Increasing sand temperatures shift the sex ratio towards females, which may, in the long term, destabilise population structure (Hawkes et al., 2007). Rising sea levels and intensified storm activity lead to erosion and more frequent inundation of nesting beaches, significantly reducing hatching success. The most vulnerable areas are small and isolated sandy stretches, known as *pocket beaches*, which in highly urbanised coastal regions often represent the last suitable nesting sites.

The study by Sella et al. (2023) demonstrated that although these *pocket beaches* account for less than 2% of the total nesting beach length in Florida, they exhibit comparable nest densities and

even higher hatching success than beaches without coastal armouring. However, modelling scenarios suggest that with continued sea-level rise and increasing frequency of extreme weather events, pocket beaches will become increasingly exposed to flooding and erosion, potentially leading to the gradual loss of suitable nesting habitats (Sella et al., 2023).

Rising ocean temperatures and changes in oceanic circulation patterns also affect the spatial and temporal distribution of food resources, which in turn alter sea turtle migration routes. These shifts directly impact their ability to locate food, synchronise migrations with optimal environmental conditions, and successfully reproduce, as demonstrated for the species *Caretta caretta* (Witt et al., 2010).

These threats do not act in isolation; their combined effects are often stronger than the impact of individual factors. For instance, the loss of nesting habitats, when combined with rising temperatures and light pollution, results in reduced reproductive success and spatial shifts in populations (Witherington et al., 2011; Vella & Vella, 2023). Therefore, effective conservation of sea turtles requires an integrated approach that combines ecological research, legislative measures, and technological innovation.

2.4 Ecological Role of Sea Turtles

Sea turtles represent key and evolutionarily ancient components of marine ecosystems, whose ecological influence extends across food webs and affects the physical structure of habitats. As widely distributed migratory species, they link oceanic and coastal environments, contributing to the transfer of energy, nutrients, and biomass between distinct ecosystems. In the past, when their populations were considerably larger, sea turtles played a crucial role in maintaining the balance of marine communities and shaping the dynamics of benthic habitats (Spotila, 2004).

From an ecological perspective, sea turtles perform several interconnected functions. They act as consumers and regulators within marine communities, for instance, green turtles (Chelonia mydas) promote the regeneration and growth of new seagrass biomass through grazing, while hawksbill turtles (Eretmochelys imbricata) feed on marine sponges, preventing their overgrowth on coral reefs (Bjorndal, 1980). Loggerhead turtles (Caretta caretta) feed on benthic invertebrates and

simultaneously provide a substrate for diverse epibiont communities, thereby enhancing species diversity in coastal habitats (Pfaller et al., 2008).

Another important function lies in the transfer of nutrients between marine and terrestrial environments. Turtles transport organic matter from feeding areas to nesting beaches, where the remains of eggs and hatchlings enrich the sand with nitrogen and carbon, supporting the growth of coastal vegetation. Their movement across the seabed further increases substrate heterogeneity and enhances nutrient cycling (Bouchard & Bjorndal, 2000).

The dynamics of feeding relationships and turtle growth can also be influenced by population density. In juvenile green turtles, high population density has been shown to reduce growth rates and body condition, indicating a direct effect of limited food availability (Bjorndal et al., 2000).

These processes highlight that sea turtles function not merely as individual consumers but as ecosystem engineers and keystone species, whose presence ensures the stability and functionality of both coastal and oceanic ecosystems. These ecological roles also extend into the broader framework of ecosystem services that sea turtles provide to both humans and natural systems (Patel et al., 2022).

In addition to their ecological functions, sea turtles play a significant role in the provision of ecosystem services, the direct and indirect benefits that their existence mediates for people and the environment. According to Patel et al. (2022), these services can be classified into four main categories: cultural, provisioning, regulating, and supporting services (Table 2).

Table 2. Summary of ecosystem services provided by sea turtles (adapted from Patel et al., 2022).

Category of Ecosystem Service	Examples of Contributions by Sea Turtles
Cultural	Cultural symbolism, identity, spiritual and educational value, diplomatic and conservation significance
Provisioning	Food resources, ornaments, traditional medicine, tourism value, natural waxes and oils
Regulating	Regulation of biodiversity, habitat modification
Supporting	Hosts for epibionts and parasites, prey for other species, biological nutrient transporters, nutrient cycling

These services demonstrate that sea turtles are not only integral components of marine food webs but also organisms that mediate numerous ecological processes and socio-cultural values. For instance, as herbivores and spongivorous predators, turtles contribute to biodiversity regulation and the maintenance of ecosystem health, while their nesting activity and nutrient transfer from sea to land represent key supporting services (Bouchard & Bjorndal, 2000; Patel et al., 2022).

From a cultural perspective, sea turtles also function as cultural keystone species, species that hold fundamental importance for the identity and traditions of local communities, and as flagship species, symbolising marine conservation efforts (Patel et al., 2022).

The availability of food and the diet may vary depending on population density and competition. At higher population densities, preferred food sources may become limited, forcing individuals to consume less optimal food and leading to reduced nutrient intake and overall condition. Empirical evidence of such a density-dependent effect has been documented in juvenile green turtles, where increased population density resulted in decreased growth rates and body condition index ($mass/length^3$), likely due to reduced food availability (Bjorndal, Bolten & Chaloupka, 2000).

2.5 Protection and Conservation in Malta

The protection of sea turtles in Malta has gained increasing importance in recent years due to the observed rise in nesting activity of loggerhead turtles (*Caretta caretta*), the only sea turtle species that regularly nests within the Maltese archipelago (Vella & Vella, 2023). While two species nest in the Mediterranean: *C. caretta* and *Chelonia mydas*, the latter is mostly confined to the eastern basin (Turkey, Cyprus, Lebanon), whereas *C. caretta* has, in recent decades, expanded its nesting range into the central Mediterranean, including Malta (Casale et al., 2018).

2.5.1. Legal Framework for Protection

At the international level, *C. caretta* is classified as Vulnerable on the IUCN Red List (Vella & Vella, 2023; IUCN, 2025). Its protection is ensured through several international conventions and regional agreements: the Convention for the Protection of the Mediterranean Sea (Barcelona Convention, Annex II), the Convention on the Conservation of Migratory Species of Wild Animals (CMS, Appendix I), the Bern Convention (Appendix II), and CITES (Appendix I) (UNEP, n.d.; CMS, 2020).

Within the European Union, the species is protected under the Habitats Directive (92/43/EEC) and is monitored as part of the Marine Strategy Framework Directive (MSFD) (Casale et al., 2018; Vella & Vella, 2024).

At the national level, *Caretta caretta* is strictly protected under the Flora, Fauna and Natural Habitats Protection Regulations (S.L. 549.44). Additionally, three Natura 2000 sites: MT0000113, MT0000115, and MT0000116, have been designated, encompassing key nesting beaches and adjacent marine areas (Vella & Vella, 2024; UNEP, n.d.).

2.5.2. Nesting Activity and Monitoring

After several decades without recorded nesting, nesting activity in Malta was re-established in 2012. Further confirmed nesting events followed in 2016 and 2018, and since 2020, nests have

been reported annually. Between 2020 and 2023, a total of 13 nests were documented across five beaches: Ramla Bay (Gozo), Għadira Bay, Golden Bay, Ġnejna Bay, and Fajtata Bay (Vella & Vella, 2023; Nature Trust, n.d.).

Monitoring and direct nest protection in Malta are coordinated by Nature Trust – Wildlife Rescue Team Malta, under the supervision of the Environment and Resources Authority (ERA). Protective measures include fencing and marking of nests, regular day and night patrols, and, when necessary (e.g., in cases of erosion or inundation), the relocation of nests to safer areas of the beach (Nature Trust, n.d.).

2.5.3. Regional Distribution and Migration Routes of Sea Turtles in the Mediterranean

The distribution of Mediterranean sea turtless is a direct reflection of their convoluted life cycle that involves islands, migratory and feeding habits over a wide range of habitats. The largest nesting sites of the loggerhead turtle (*Caretta caretta*) are predominantly located in the southeastern part of the region, notably in Turkey, Greece, Cyprus, and Lebanon, while the green turtle (*Chelonia mydas*) lays eggs only on the eastern Mediterranean coast (Figure 6.) (Casale et al., 2018).

Sea turtles travel long distances between the beaches where they nest and the areas where they feed. The neritic zones of continental shelves, for example, those off southern Italy, Tunisia, Egypt, Turkey, and Cyprus, are the main feeding and overwintering grounds for both species (Figure 7.). Mature turtles then embark on long-distance journeys via the central and eastern Mediterranean most of Malta is, therefore, a place connecting the routes but at the same time, a feeding area as well (Figure 8.) (Casale & Tucker, 2017).

Comprehending sea turtles' migratory routes as well as their seasonal movements is a must if the conservation of these animals is to be adequately planned. This knowledge then makes it possible to locate those areas where there is a spatial-temporal overlap between the turtles and human activities, such as heavily industrialized fishing or the building up of the coast, which are the main sources of probable encounters between man and turtle.

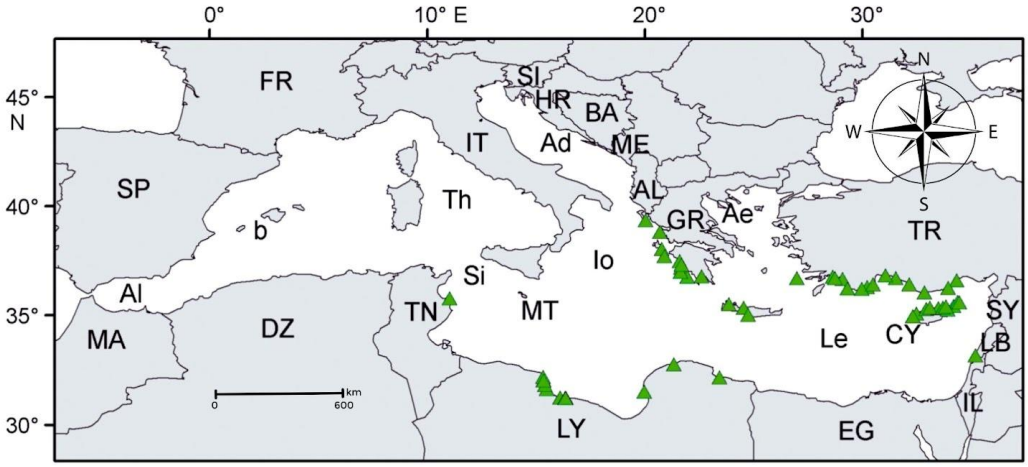

Figure 6. Main nesting sites of loggerhead turtles (Caretta caretta) in the Mediterranean Sea. Locations with more than 10 nests per year and a density of at least 2.5 nests per kilometre of coastline are shown. Abbreviations indicate individual countries and marine areas. Adapted from Casale & Tucker (2017).

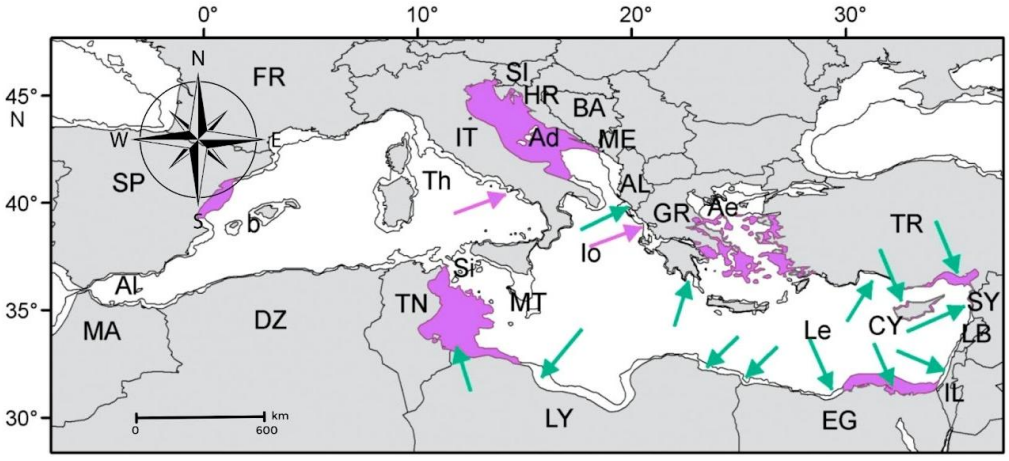

Figure 7. Coastal (neritic) areas used by the loggerhead turtle (Caretta caretta, in purple) and the green turtle (Chelonia mydas, in green) for foraging and overwintering. These areas correspond to continental shelves delineated by the 200 m isobath. Adapted from Casale & Tucker (2017).

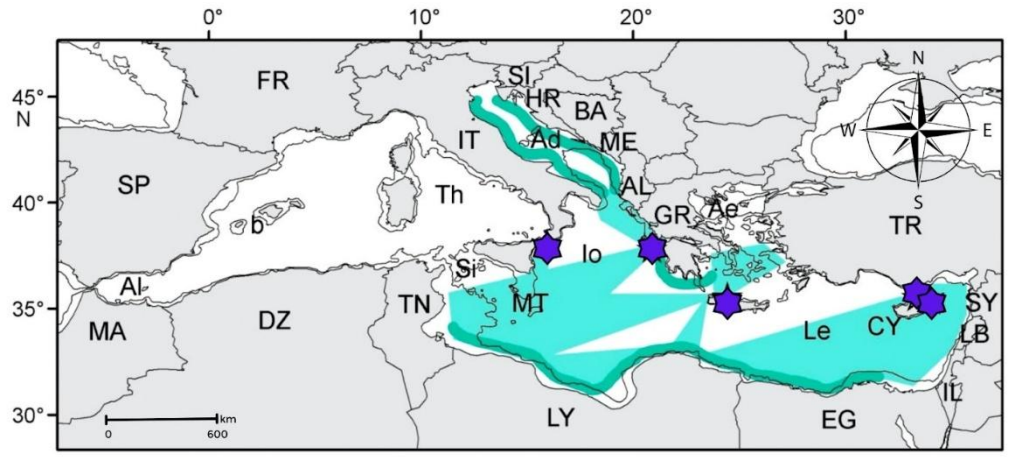

Figure 8. Primary migratory routes of adult loggerhead turtles (Caretta caretta), including both females and males, during reproductive migrations to and from breeding areas ( ). Blue areas indicate migrations in open waters, while darker bands along the coast represent routes in shallow waters. Adapted from Casale & Tucker (2017).

2.5.4. Conservation Management and Public Involvement

Most of the conservation works in Malta are done together with Nature Trust Malta members who are trained and volunteers who help with patrolling, recording, and releasing of hatchlings. The emphasis is mainly on lessening the disruption of nests and educating the public on the conservation of sea turtles (Nature Trust, n.d.).

Thanks to these measures, recent years have seen an increase in hatching success and hatchling survival rates, consistent with similar trends observed in other areas of the central Mediterranean (Casale et al., 2018).

2.6 Geomorphology of Maltese Beaches and Relevance for Nesting

The Maltese Archipelago is situated in the central Mediterranean Sea, to the south of Sicily, at the conjunction of the African and Eurasian tectonic plates. After the formation of the Sicilian fold-and-thrust belt at the end of the Messinian Salinity Crisis, approximately five million years ago, the area experienced extensional deformation that created two almost perpendicular fault systems which continue to shape the geomorphology of the Maltese Islands (Rossi et al., 2025). The Sicily Channel Rift Zone consists of three main grabens, the Pantelleria, Linosa, and Malta grabens, that have been active since the Late Miocene and have influenced both sediment deposition and the development of the Gela foredeep (Rossi et al., 2025).

The Maltese Archipelago located in the central Mediterranean Sea south of Sicily is a geological structure indebted to the ongoing tectonic processes. The tectonic forces over geological time have converted the region from a single vast basin into a set of depressions and rift zones with the most famous ones being the Malta Graben and the Pantelleria Rift Zone which characterize the seafloor around Malta (Prampolini et al., 2017). The geomorphology of the islands as of today is an outcome of this intricate geological setting: the shores are mainly rocky, and only a few sandy bays exist. These sandy beaches, though few, serve as appropriate nesting places for the loggerhead turtle (Caretta caretta). Figure 9 shows where Malta is in this tectonic and geomorphological framework.

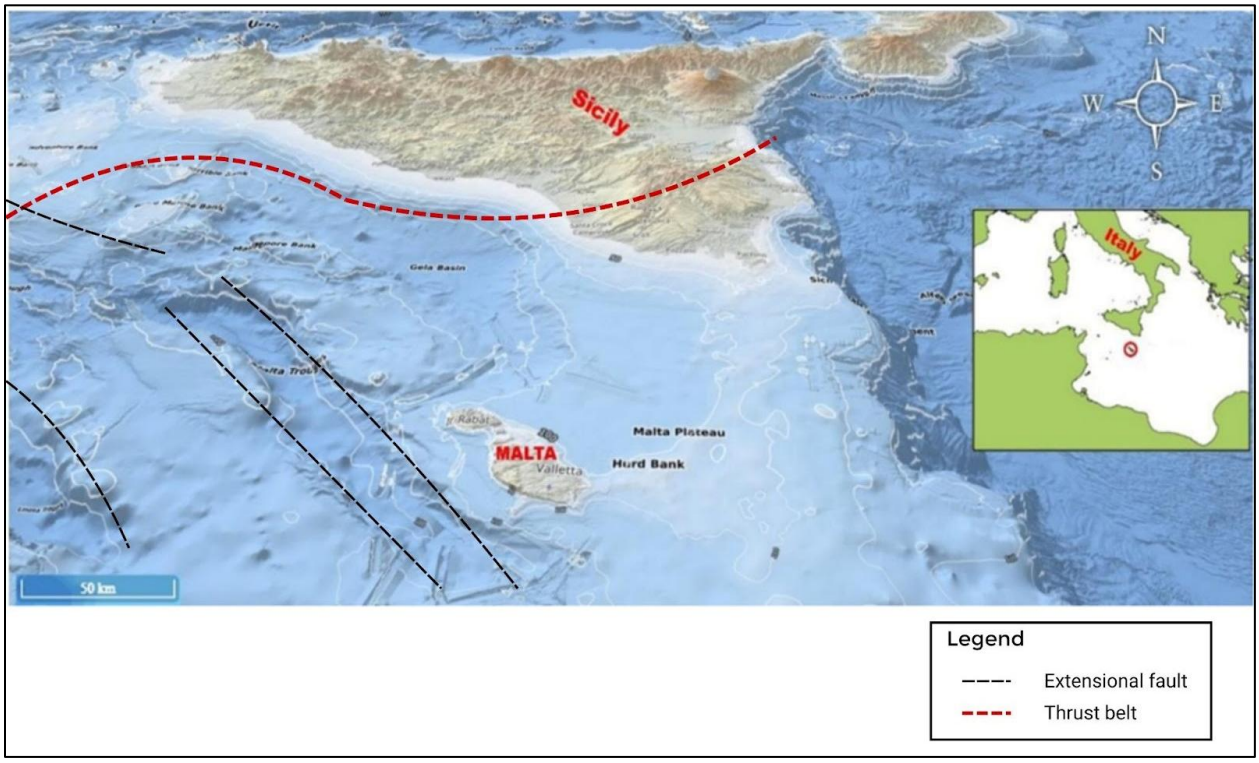

Figure 9. Geographic and tectonic setting of the Maltese archipelago within the central Mediterranean Sea. The 3D bathymetric model was adapted from Colica (2022) and Prampolini et al. (2017). The inset map shows the position of Malta within the Mediterranean basin. (Derived product from the GEBCO 2020 Grid).

Sandy coves situated between rocky coastal sections, known as pocket beaches, represent important habitats for coastal fauna, including sea turtles. In highly urbanized regions, similar small sandy stretches, often bordered by reinforced coastal structures (coastal armouring), are referred to as urban pocket beaches. Despite their limited area, these beaches can provide essential nesting, feeding, and resting grounds, particularly in regions where most natural beaches have been lost due to construction or erosion (Sella et al., 2023).

From a geomorphological perspective, pocket beaches are narrow sedimentary environments with limited sand supply, shallow substrate depth, and low dune profiles, which makes them highly susceptible to erosion and inundation during storms. Nevertheless, they may still offer suitable nesting conditions for sea turtles if the sand retains its natural composition and the nesting area remains at a sufficient distance from the swash zone (Sella et al., 2023).

The Maltese coastline is predominantly rocky, with only a few sandy segments found mainly along the northwestern and southeastern parts of the islands. Bays such as Għadira Bay, Golden Bay, Għajn Tuffieħa Bay, and Ġnejna Bay represent, from a geomorphological standpoint, limited but ecologically valuable areas with potential for loggerhead turtle (*Caretta caretta*) nesting. The sand in these bays is primarily carbonate in composition and is characterised by high permeability and low moisture content, which promotes gas exchange but increases the risk of nest overheating during heatwaves (Prampolini et al., 2017; Vella & Vella, 2023). The absence of dune vegetation further reduces substrate stability and increases vulnerability to erosion and slumping (Prampolini et al., 2018).

The northwestern coast of Malta, where most of the sandy bays suitable for sea turtle nesting are located, is characterised by narrow sedimentary basins bordered by limestone ridges and steep slopes (Figure 10.) (Prampolini et al., 2017).

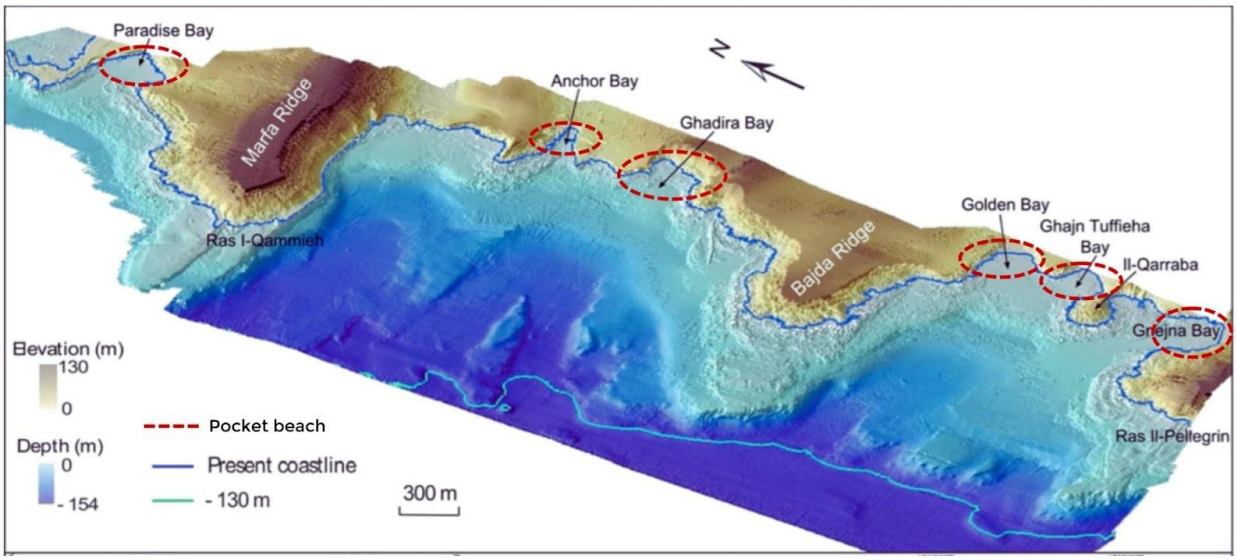

Figure 10. 3D model of the northwestern coast of Malta showing the main sandy bays: Paradise Bay, Għadira Bay, Golden Bay, Għajn Tuffieħa Bay, and Ġnejna Bay. The topography highlights the characteristic pocket beach morphology of the Maltese coastline. Adapted from Soldati et al. (2019).

In the context of Malta, where the coastline is highly urbanised and natural sandy beaches constitute only a small fraction of the total shoreline, these small natural coves may serve as critical refugia for sea turtle nesting. The study by Sella et al. (2023) suggests that such *pocket beaches*

may exhibit comparable or even higher hatching success rates than larger beaches, provided they are not subject to mechanical disturbance or coastal armouring. Therefore, maintaining their geomorphological stability and protecting them from development are essential for the long-term preservation of loggerhead turtle (*Caretta caretta*) nesting populations in the Mediterranean region.

2.7. Ground Penetrating Radar

The Ground Penetrating Radar (GPR) method, illustrated in Figure 12, is now commonly used in geophysical and geological surveys (Annan, 2009). The principle is based on transmitting high-frequency electromagnetic waves into the subsurface and analyzing changes in the reflected signal.

This technique can be applied across a wide range of environments, from natural geological formations to artificial materials such as concrete or asphalt. Owing to the variability of materials and frequencies that can be used during measurement, GPR offers a broad spectrum of applications in geophysics. It is frequently employed in glacial, periglacial, and fluvial environments, as well as in desert regions, to investigate the structure of glaciers, permafrost, and sediments, or to determine the depth of groundwater tables (El-Said, 1956).

Although research on the propagation of radio waves above the Earth's surface advanced significantly during the first half of the 20th century, the first practical applications of GPR emerged in the second half. One of the pioneers was El-Said (1956), who used electromagnetic waves to study groundwater in the Egyptian desert and determined its depth based on reflected signals, which he later confirmed by drilling tests. Since then, the GPR method has undergone substantial development, has been validated in numerous studies, and has become a reliable tool for geophysical analysis. Modern approaches also focus on inverse data interpretation, in which the electrical properties of materials are derived from the reflected waveforms (Kruk et al., 2003).

GPR's physical principle is based on the utilization of radio waves for "probing the ground," in other words, identifying the boundaries of materials that have different dielectric properties (Figure 11.). The apparatus includes a transmitter, which finally produces short electromagnetic pulses, and a receiver, which records the reflections from the parts of the ground. The variations

in the reflected signal depend upon the kind and the depth of the material being studied, and this signal is then transformed into a radargram, which shows the vertical cross-sections of the subsurface (Annan, 2009).

Due to its wide frequency range, GPR can be used in many types of environments. The use of low-frequency antennas (e.g., 200-400 MHz) enables deeper penetration, while the use of high-frequency antennas (900-1000 MHz) allows getting more detailed images of the top layers. Such versatility turns GPR into an instrument suitable for a vast range of different applications, which are not only geological and glaciological research but also the non-destructive testing of construction materials (Bristow & Jol, 2003).

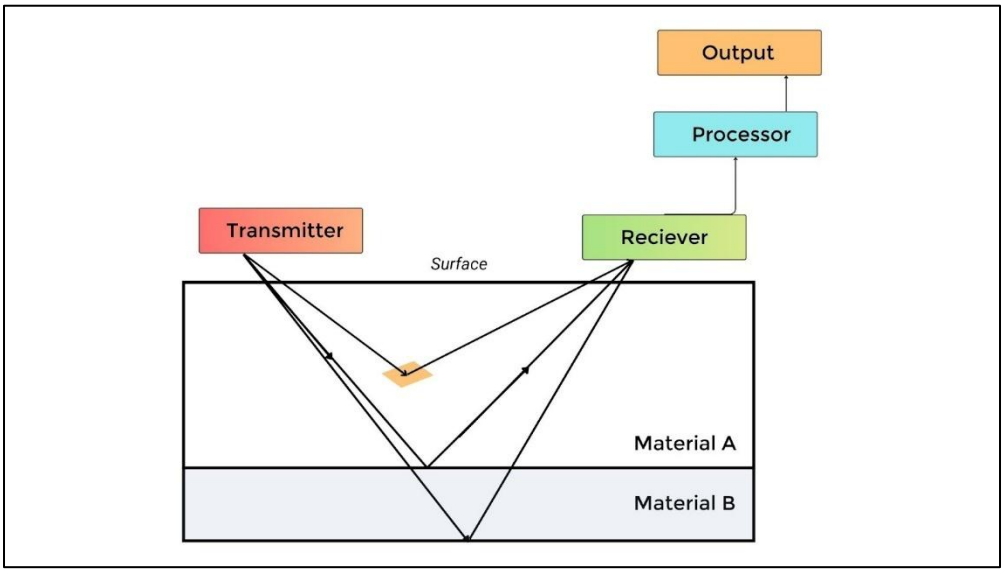

Figure 11. Principle of testing with the GPR system Adapted from Dong & Ansari, (2011).

Figure 12. Ground penetrating radar (Emanuele Colica, 2025).

2.8. Photogrammetry and LiDAR Technologies

Photogrammetry is a discipline that deals with obtaining quantitative information from image data, most often from photographs. According to Pavelka (2003), it is a scientific and technical approach that enables the creation of maps, digital terrain models, and other measurable products derived from image records. Aber et al. (2010) add that the main goal of photogrammetry is to accurately determine the shape and spatial arrangement of objects or the Earth's surface based on the analysis of two-dimensional images. This method is widely used to determine coordinates, measure distances, areas, and volumes, as well as to create maps and three-dimensional digital models.

Pavelka (2003) points out that photogrammetry has a tradition dating back more than 150 years – from analog methods of terrestrial intersection photogrammetry to today's digital approaches based on automated image processing. Major technological advances include the development of stereoscopy, aerial photography, and later the use of UAV (Unmanned Aerial Vehicle) platforms, which have made it possible to capture detailed image data from low altitudes.

Depending on the position of the observation point, we distinguish between:

- Ground (close) photogrammetry, where the observation point is stationary and located on the earth's surface. This approach is often used for documenting smaller objects.

- Aerial photogrammetry, where the imaging device is located in an aircraft, drone, or other flying vehicle. This method is suitable for larger areas but requires accurate georeferencing and calibration.

- UAV photogrammetry, which from a technical point of view falls between aerial and close-range photogrammetry, as it combines the advantage of an aerial view with the detail of close-range imaging (Aber et al., 2010).

In terms of the number of images evaluated, we distinguish between single-image photogrammetry, which allows measurement only in a plane, and multi-image photogrammetry, which allows the reconstruction of a three-dimensional object thanks to overlapping images. Currently, the most commonly used method is Structure from Motion (SfM), which combines elements of stereophotogrammetry and intersection photogrammetry and enables automatic 3D reconstruction of objects (Mířijovský, 2013).

Modern technologies extend photogrammetry with the principles of LiDAR (Light Detection and Ranging), which uses laser beams to measure distances instead of optical images. By combining photogrammetric images with LiDAR data, higher accuracy of 3D models can be achieved, especially when documenting complex structures. In recent years, mobile photogrammetry has also been developing, which uses integrated sensors in smart devices for photogrammetric reconstruction supplemented by depth data from LiDAR. This technology enables detailed 3D documentation of smaller objects and is therefore also used in environmental studies focused on non-invasive monitoring of terrain structures and biological objects (Shan & Toth, 2008).

2.9. Artificial Intelligence and Computer Vision for Object Detection

In recent years, machine learning and artificial intelligence (AI) technologies have become essential tools for processing image data, particularly in the field of computer vision. These approaches enable the automatic recognition and localization of objects in images, replacing time-consuming manual methods and improving detection accuracy (Zhao et al., 2019; Zou et al., 2023). The principles of these methods can also be applied in environmental research, for example, to identify animal tracks or other natural features in field imagery.

2.9.1 Development of Object Detection Methods

The development of object detection methods can be divided into two main periods, traditional approaches and deep learning-based approaches. Traditional methods (e.g., the Viola–Jones detector, the HOG detector, Histogram of Oriented Gradients, and the Deformable Part-Based Model (DPM)) relied on manually defined image features selected by experts (Viola & Jones, 2001; Dalal & Triggs, 2005; Felzenszwalb et al., 2008). These algorithms enabled the first automatic real-time object detection systems; however, their accuracy and ability to generalise across environments were limited (Zou et al., 2023).

A major breakthrough occurred after 2012 with the advancement of deep learning and the development of Convolutional Neural Networks (CNNs), which are capable of automatically extracting features from image data (Zhao et al., 2019). CNNs consist of convolutional layers, non-linear activation functions (e.g., ReLU), pooling layers, and fully connected layers. Through this hierarchical structure, the model learns to recognise visual patterns, from basic edges and shapes to complex structures (Tammina, 2019).

2.9.2 Principle of the YOLO Method

The YOLO (You Only Look Once) model, introduced by Redmon et al. (2016), brought an entirely new approach to object detection. Unlike earlier systems that relied on reusing classifiers (e.g., R-CNN – Region-based Convolutional Neural Network or DPM - Deformable Part-Based Model), YOLO treats object detection as a regression problem, directly mapping an input image to bounding box coordinates and class probabilities.

The input image is split up into a grid of S × S cells by the network. The cells are those which output objects whose centre is within the cell. The model predicts a few bounding boxes for each cell and gives them a confidence score, the score indicating both the probability that a certain box contains an object and the accuracy of the box in terms of the size and shape of the object. At the same time, the network calculates probabilities for each object class separately and those probabilities multiplied by the confidence scores give the final score for every box.

By using the proposed method, the whole image can be processed in one go through the neural network which unifies all the computations. Consequently, YOLO is able to carry out 45 operations (where each operation corresponds to one frame) per second thus allowing for real time detection even in video sequences (Redmon et al., 2016). The small network version known as Fast YOLO is reported to perform at a speed of up to 155 frames per second and at the same time, it is twice as accurate as the previously existing real-time detection methods.

Another kye feature of YOLO is that it perceives the image in a more comprehensive way - it considers all objects at the same time instead of dealing with individually cropped regions. Thus the model is able to utilize the context of the scene more effectively and also identify genuine objects from the noise of the background. In their work, Redmon et al. (2016) showed that YOLO is far less likely to mistakenly detect the background as objects than is the case with region-based methods like Fast R-CNN.

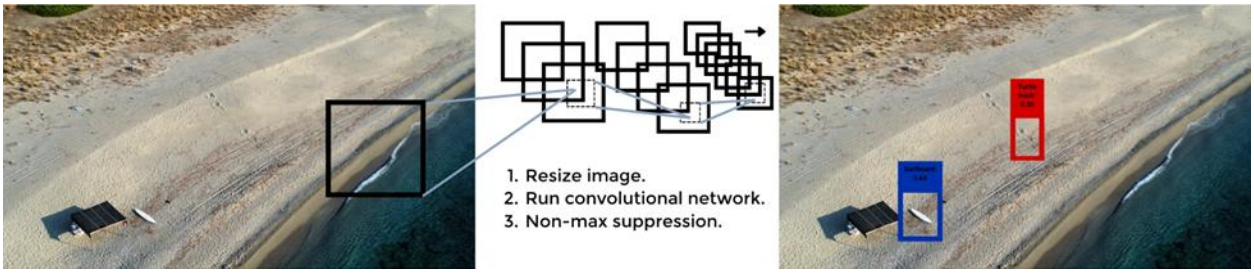

Figure 13. Principle of the YOLO object detection system, adapted from Redmon et al. (2016). The model divides the input image into a grid, applies a single convolutional neural network to predict bounding boxes and class probabilities, and identifies objects based on confidence thresholds.

Processing an image using the YOLO model is relatively simple and straightforward. First, the input image is resized to a resolution of 448 × 448 pixels; then, the entire image is processed by a single convolutional neural network, and finally, the resulting detections are filtered according to the model's confidence score. The diagram illustrates the basic steps of object detection within this method. Figure 13 shows the fundamental stages of the detection of objects by this technique.

3. Methodology

3.1 Study Area and Nest Simulation

The experiment was conducted at Golden Bay beach (Figure 14. and Figure 15.), which is located on the northwestern coast of Malta and is one of the most popular sandy beaches of the island. To avoid disturbance from beach visitors from interfering and to ensure that the work could go on uninterrupted, the fieldwork was done at 5:00 a.m. Golden Bay is a pocket beach located in a rocky bay, where sediment is naturally deposited between the rocky outcrops. The beach is quite accessible and features a gentle slope from the shore, thus making it an ideal place for sea turtles to lay their eggs.

Figure 14. Map of Malta showing the study area.

Figure 15. Detailed view of the study area.

Since sea turtle nesting in Malta occurs only sporadically and no active nests were recorded during the research period, a simulated nest was created for the purposes of the experiment. Access to real nests would not have been ethically acceptable; therefore, the simulation was designed to avoid any disturbance to the natural nesting activity of turtles.

An experimental plot measuring 6 × 6 meters was marked out 10 meters from the waterline (Figure 16.). The nest was constructed by digging a tunnel-shaped shaft with a diameter of 17 cm to a depth of 52 cm, which then widened into a spherical chamber with a diameter of 30 cm. At this depth, the sand was noticeably denser and more humid, allowing the chamber to maintain its shape.

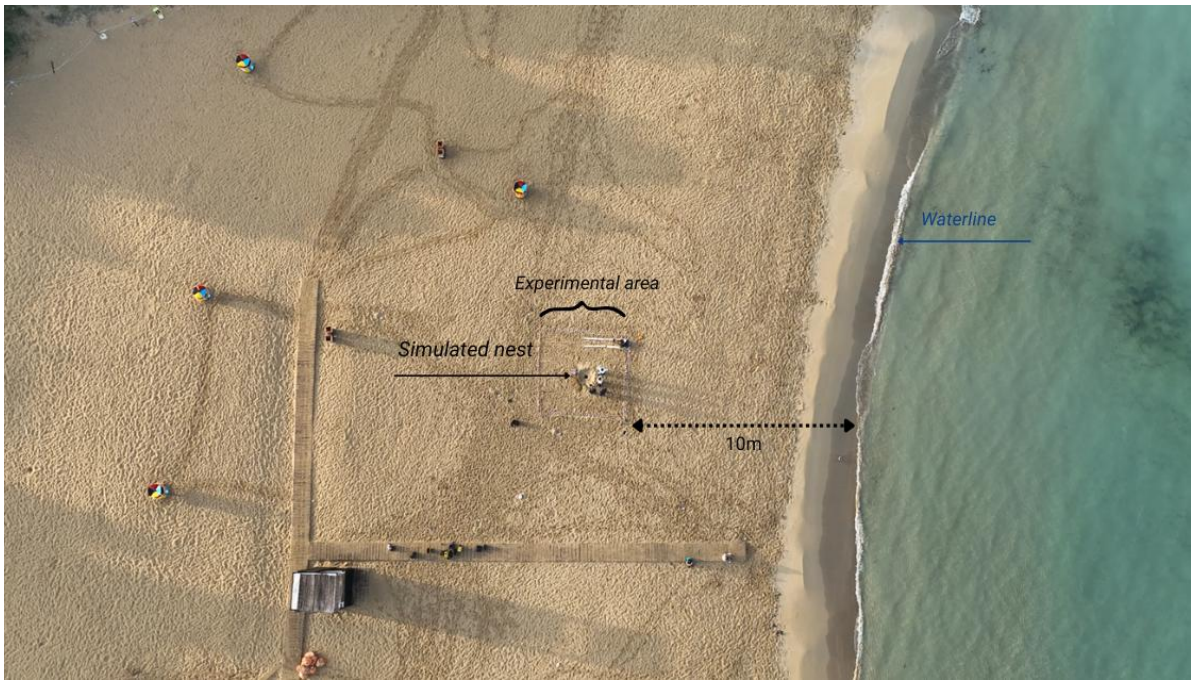

Figure 16. Study site showing the 6 × 6 m experimental area located approximately 10 m from the waterline, including the position of the simulated turtle nest used for testing.

While creating a simulated nest, the typical sizes of a loggerhead turtle (*Caretta caretta*) nest, which were taken from the studies, have been considered. Najwa-Sawawi et al. (2021) defined standard parameters of nest morphology, including chamber depth, “bowl” diameter, and “neck” diameter (see Figure 17. A). These parameters were taken into account when replicating the nest

structure to ensure that the simulation closely resembled the natural nesting conditions reported in scientific literature.

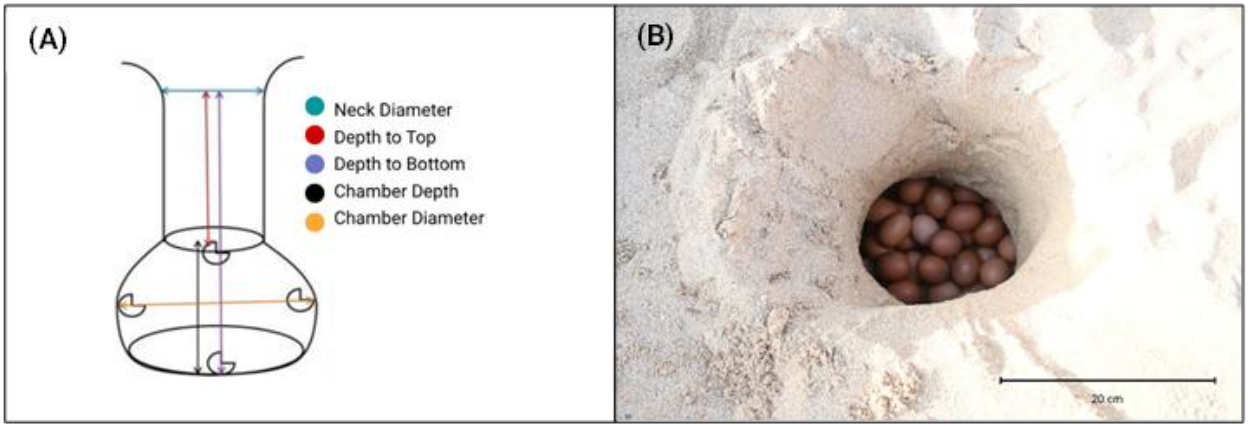

Figure 17. (A) Measurement of nest depth using a weighted line (adapted from Najwa-Sawawi et al., 2021). (B) Simulated turtle nest with chicken eggs used for GPR testing.

Fifty-four chicken eggs were randomly placed inside the chamber and subsequently covered with sand. This number approximately corresponds to the average clutch size of the loggerhead turtle (*Caretta caretta*), thereby maintaining the overall volume of the nest cavity. Chicken eggs were selected for their similarity in size and shape to sea turtle eggs, although turtle eggs are slightly softer and rounder, resembling ping-pong balls in appearance. Throughout the entire experiment, photographs were taken to document each phase of the procedure (Figure 17. B).

3.2 3D Reconstruction of Simulated Nest Interiors

In the following phase of the experiment, a 3D reconstruction of the internal structure of the simulated sea turtle nest was conducted. The aim was to visually capture the arrangement of the eggs and the overall dimensions of the chamber. These data were later used as a reference for the accurate interpretation of Ground Penetrating Radar (GPR) readings.

The 3D scanning was performed using Scaniverse (version 5.1.0; Niantic, Inc.), a mobile application that combines photogrammetric reconstruction with LiDAR (Light Detection and Ranging) technology to generate highly accurate three-dimensional models of the surrounding

environment. The entire nest was documented with the mobile device's camera (refer to Figure 18). The scanning was facilitated by the iPhone 12 Pro Max's integrated dToF (direct Time-of-Flight) LiDAR sensor, which operates at a physical range of up to 5 meters. This system provides a spatial resolution with an error margin typically within 1% of the distance from the object, ensuring sub-centimeter precision for close-range documentation of the nesting chamber. By integrating LiDAR depth data with photogrammetric image processing, the system generates a dense point cloud and a textured 3D mesh with high spatial accuracy. The camera went through the tunnel and into the egg chamber, rotating in a circular motion to capture the structure from all possible angles. To ensure accuracy of the reconstruction, the scanning procedure was repeated several times.

Figure 18. Scanning of the simulated sea turtle nest using a mobile application employing LiDAR technology. The device was used to capture the internal structure and wall texture of the nesting chamber.

The data were pre-processed within the mobile application, which generated a basic 3D model (mesh). This model was subsequently exported and further refined using the computer software CloudCompare (version 2.13.2; CloudCompare, 2024). The resulting 3D reconstruction displays the nest walls and chamber along with the spatial arrangement of the eggs. For visual verification, the number of visible eggs in the model was compared with the actual number placed in the nest, thereby confirming the accuracy of the reconstruction.

Although this method proved useful, 3D reconstruction of the nest interior using a mobile application has certain limitations. Since the camera was operated manually, minor inaccuracies may have occurred due to irregular hand movement. Furthermore, this approach is limited to small-scale objects such as a single nest and cannot be applied to larger areas, such as entire beaches. Therefore, this technique should be considered primarily as a tool for qualitative documentation rather than as a predictive method.

3.3 Ground Penetrating Radar (GPR)

Another method used in this study is Ground Penetrating Radar (GPR), a non-invasive geophysical technique that can be used to detect sea turtle nests (Ermakov et al., 2012). The experiment was conducted at the previously described site, Golden Bay, where the simulated turtle nest was created.

GPR, also known as impulse radar, subsurface radar, or ground radar, is a method used to detect variations in the electrical properties of the shallow subsurface. While the technique is capable of reaching depths of up to about 50 meters in favorable conditions (Neal, 2004), the effective penetration depth depends strongly on the antenna frequency and substrate characteristics. In this study, a Proceq GPR employing Stepped-Frequency Continuous-Wave technology was used, operating within a modulated frequency range of 40–3440 MHz. Given this high-frequency range and the fine, dry sandy substrate of Golden Bay, the system was optimized for high-resolution detection within the upper 1 meter, corresponding to the expected depth of a sea turtle nest.

The principle of operation is based on emitting high-frequency electromagnetic pulses that penetrate the substrate, reflect off buried structures or materials, and are subsequently recorded by a receiver (Neal, 2004). In the context of this experiment, the target objects were eggs placed

within the sand chamber. Ermakov et al. (2012) published a study demonstrating the effectiveness of GPR in detecting sea turtle eggs.

For the purposes of the experiment, a 6 × 6 m area was marked out on the beach, and the right angle was verified using the practical application of the Pythagorean theorem ($a^2 + b^2 = c^2$), where a triangle with sides of 3 m, 4 m, and 5 m forms an exact 90° angle (Figure 19.).

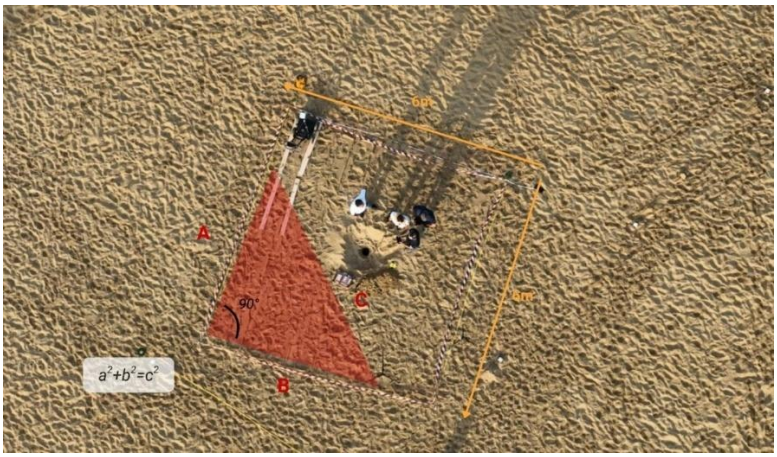

Figure 19. Study site showing the 6 × 6 m experimental area marked on the beach, with the right angle established using Pythagoras' theorem.

The GPR measurements were conducted in a regular serpentine pattern. The device was guided from the lower left corner vertically upward, then shifted one step to the right and moved downward again. Each pass of the scanner thus covered one vertical section of the surveyed area. In this way, a grid with a spacing of approximately 20 cm was created, ensuring consistent coverage of the entire site. This movement was repeated until the entire square area was scanned. To increase the reliability of the results, the entire site was scanned twice. The sand was fine and

dry, providing suitable conditions for measurement. To prevent the wheels of the GPR unit from sinking into the sand, two long wooden slats were placed beneath them (Figure 20.).

Figure 20. GPR survey conducted in the designated experimental area.

While the GPR method focuses on detecting subsurface structures, the recognition of sea turtle tracks on the beach surface represents another crucial step in locating potential nests. For this purpose, a method based on artificial intelligence (AI) was tested, specifically using the MakeSense AI software platform for image annotation and model training.

3.4 Detection of Sea Turtle Tracks Using Artificial Intelligence (AI)

Turtle tracks are the primary visual indicator of the presence of sea turtle nests and are therefore a key element in identifying potential nesting sites. However, identifying those tracks in the field consumes a lot of time and it is a very subjective task as the person's experience, lighting conditions and sand texture influence the results. Therefore, a method based on artificial intelligence (AI) has been implemented with a goal to automate the process of finding turtle tracks on the ground and drone images.

To develop a functional model, it is first necessary to collect and annotate an extensive dataset of images on which the machine learning algorithm can be trained. Within this project, two main datasets were utilized.

The first dataset was provided by the University of Cádiz (Spain) and included 22 aerial drone images of beaches with visible sea turtle tracks. These images primarily captured the characteristic shapes of the tracks and “drag marks” in their natural environment.

The second dataset originated from the non-profit organization Nature Trust Malta, which provided 132 photographs taken during both night patrols and daytime monitoring. These images depict turtle tracks from various angles and under different lighting conditions. Some were taken under red light (Figure 21.), which volunteers use to avoid disorienting or stressing turtles during nesting. Monitoring is carried out during the nesting season, when female loggerhead turtles (*Caretta caretta*) come ashore on Maltese beaches to lay their eggs. Automating this process would, in the future, significantly improve the efficiency of fieldwork conducted by volunteers.

All available photographs were subsequently uploaded to the web-based platform MakeSense.ai, which enables manual annotation of image data. On each image, individual objects were marked using bounding boxes, with each category assigned a separate label (Figure 21.).

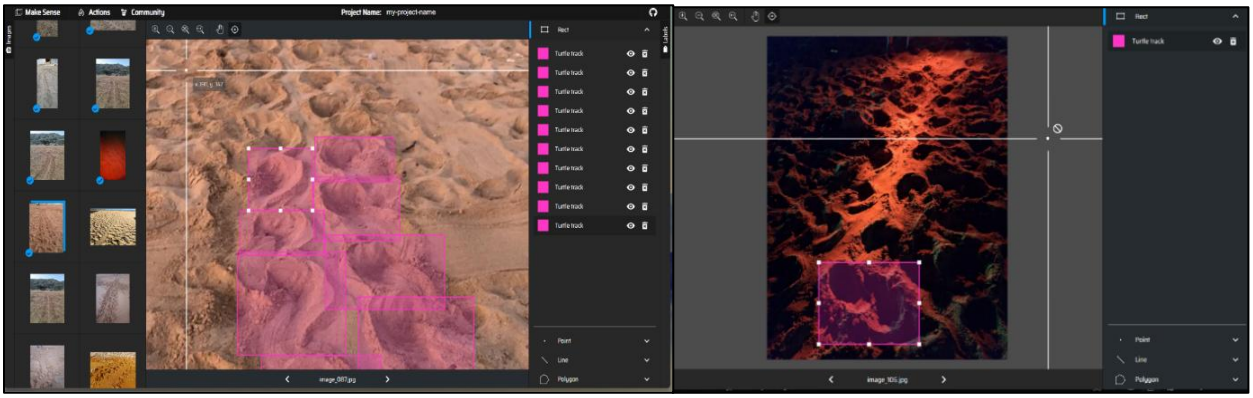

Figure 21. Screenshots from MakeSense.ai showing the manual annotation of sea turtle tracks.

In addition to the turtle tracks themselves, other relevant elements were also annotated, such as boats, rocks, people, tents, garbage bins, and potential nest-shallow depressions at the end of the tracks that may indicate an attempted egg-laying event (Figure 22.).

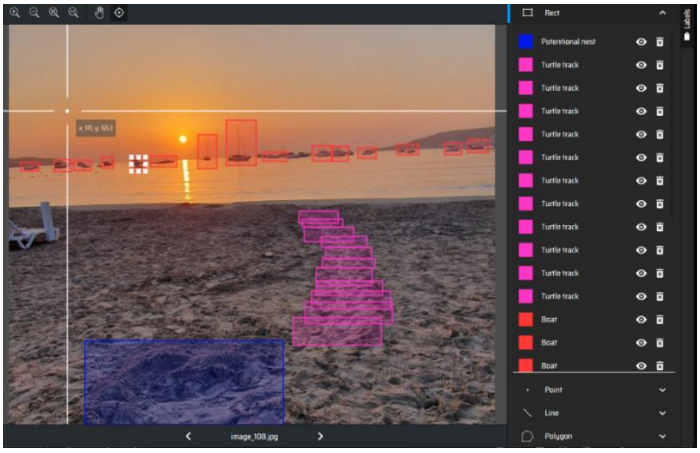

Figure 22. Screenshot from MakeSense.ai showing the annotation of turtle tracks and other relevant features, including boats, rocks, people, tents, garbage bins, and potential nesting depressions.

Expanding the dataset to include multiple categories allows verification of whether the detection algorithm can correctly distinguish turtle tracks from other visually similar objects, thereby reducing the risk of false detections. After completing the annotation process, all datasets were exported in the YOLO (.txt) format, which is commonly used for training convolutional neural networks (CNNs) designed for object detection.

Examples of the photographs used for model training, together with their annotated versions and YOLO label files, are presented in Table 3. These examples illustrate the workflow of data preparation prior to model training in MakeSense.ai.

Table 3. displays the examples of the pictures utilized for the model training along with their annotated versions and YOLO label files. These examples represent the data preparation process before model training in MakeSense.ai.

	(A) Original image	(B) Annotated image (MakeSense.ai)	(C) YOLO label file (.txt)
Image_060		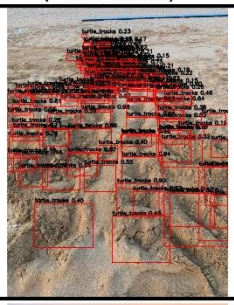	1 0.707885 0.824117 0.483359 0.216590 1 0.623912 0.674347 0.282642 0.125960 1 0.671019 0.572197 0.311316 0.099846 1 0.655658 0.490015 0.268305 0.086022 1 0.641321 0.419355 0.206861 0.064516 1 0.632104 0.375576 0.217102 0.078341 1 0.648490 0.328725 0.213006 0.061444 1 0.645417 0.286482 0.186380 0.050691 1 0.634153 0.260369 0.196621 0.026114 1 0.601382 0.247312 0.167947 0.046083 1 0.561444 0.227343 0.141321 0.043011 1 0.541987 0.207373 0.176139 0.043011 1 0.491807 0.174347 0.112647 0.029186 1 0.455965 0.157450 0.118792 0.035330 1 0.455965 0.142089 0.094214 0.029186 1 0.231695 0.734255 0.309268 0.218126 1 0.267537 0.559140 0.121605 0.129032 1 0.340246 0.457757 0.227343 0.086022 1 0.385305 0.400922 0.178187 0.073733 1 0.406810 0.339478 0.172043 0.064516 1 0.432412 0.302611 0.178187 0.058372 1 0.417051 0.266513 0.098310 0.041475 1 0.399642 0.241167 0.120040 0.027650 1 0.368920 0.215822 0.083973 0.041475 1 0.348438 0.188172 0.104455 0.038402
Image_042		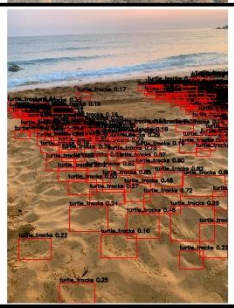	1 0.834869 0.728111 0.172043 0.122888 1 0.715054 0.677419 0.206861 0.095238 1 0.579877 0.639785 0.169995 0.096774 1 0.487711 0.596006 0.137225 0.061444 1 0.413357 0.563894 0.118987 0.057787 1 0.358740 0.525126 0.118987 0.043157 1 0.303148 0.495136 0.097530 0.029990 1 0.283642 0.468071 0.076073 0.034379 1 0.256821 0.441007 0.073148 0.032916 1 0.177822 0.453076 0.078999 0.027796 1 0.194402 0.485627 0.078999 0.024139 1 0.229025 0.527686 0.093629 0.036574 1 0.271451 0.563529 0.125814 0.055592 1 0.335133 0.607783 0.118987 0.044620 1 0.400678 0.641065 0.132641 0.055592 1 0.611343 0.732499 0.138493 0.068759 1 0.870773 0.603906 0.175554 0.099481 1 0.683515 0.562212 0.214566 0.078999 1 0.555263 0.526004 0.114110 0.037305 1 0.508449 0.499305 0.118011 0.030722 1 0.446517 0.481018 0.118987 0.033648 1 0.415795 0.456880 0.110209 0.029259 1 0.387024 0.438593 0.124838 0.036574
Image_107			1 0.570661 0.849462 0.249872 0.298003 1 0.616743 0.594470 0.317460 0.150538 1 0.245008 0.640553 0.294931 0.202765 1 0.385305 0.453149 0.178187 0.125960 1 0.462110 0.336406 0.163850 0.095238 1 0.462110 0.236559 0.122888 0.110599 1 0.681260 0.447773 0.208909 0.149002 1 0.669995 0.307220 0.215054 0.165899 1 0.680236 0.192780 0.161802 0.084485 1 0.652586 0.122888 0.147465 0.073733 1 0.620840 0.064516 0.153610 0.061444 4 0.272657 0.122888 0.194572 0.092166

The exported text files contain the coordinates of the bounding boxes and the corresponding object class. Based on these data, a training dataset was created and subsequently used for the development and testing of the model described in the following chapter (3.4.1).

In the future, this system could be implemented for the automated analysis of images captured by drones or cameras installed directly on the beach, allowing continuous monitoring of turtle track occurrences without the need for an observer's physical presence. Such an approach would not only improve monitoring efficiency but also minimize human disturbance in sensitive nesting habitats.

3.4.1 Model Training and Validation

The annotated dataset was used to train an object detection model based on the YOLOv8 (You Only Look Once) architecture. Training was performed using supervised learning on the labelled images created in MakeSense.ai. While the initial dataset consisted of 154 images, a subset of 36 representative images was selected for the manual annotation and supervised learning phase due to the specific requirements for high-quality ground-truth data. The dataset was randomly split into training and validation subsets, allowing the evaluation of model performance during learning. The remaining 118 images from the original pool were reserved as a separate test set to evaluate the model's performance on unseen data. Due to the limited dataset (36 labelled images), a pre-trained YOLOv8 model was used and fine-tuned to this specific task.

Several key hyperparameters were optimized, including image resolution, batch size, number of epochs, and confidence and IoU (Intersection over Union) thresholds. During each iteration, the model's predictions were compared with the ground-truth bounding boxes to minimize detection errors and update the model weights accordingly. The best-performing weights were selected based on validation performance.

The labelled images included six object classes: turtle tracks, people, rocks, boats, bins, and potential nests, with a strong class imbalance, as most annotations corresponded to turtle tracks. Figure 22 illustrates the distribution of labels across the dataset, showing that most bounding boxes are concentrated in the central region of the images and are relatively small.

3.5 Integration of Methods

The combination of the applied methods represents a crucial step toward achieving more accurate and reliable results. Individually, each technique: LiDAR, GPR, and AI detection - provides only partial information about the location and characteristics of a nest; however, their integration enables a comprehensive understanding of both surface and subsurface features. This integrated

approach allows for a more efficient narrowing of the survey area while minimizing any potential disturbance to the nest.

LiDAR provides detailed spatial data on the shape and structure of the nest surface, capturing microtopographic features and identifying potential nesting microhabitats. GPR (Ground Penetrating Radar) complements these data by supplying information from subsurface layers and detecting anomalies that may correspond to an egg chamber. AI detection (using the MakeSense AI platform) focuses on surface indicators, primarily the identification of turtle tracks, which serve as visual cues for locations where females have emerged onto the beach and possibly initiated nesting.

By integrating these three methods, a comprehensive system for non-invasive nest detection is established. The AI model can identify turtle tracks from photographs or drone imagery and highlight areas with the highest probability of nest presence. Detailed GPR measurements can then be conducted in those areas to confirm the presence of subsurface anomalies. The GPR scan results can subsequently be compared with LiDAR-derived topographic data to better understand the relationship between beach morphology and nest placement.

This integrated approach offers several advantages: it enhances the accuracy of nest localization, reduces the area that must be physically surveyed, and enables the standardization of monitoring procedures in conservation practice. Moreover, it provides a spatial framework in which multiple data layers can be combined and visualized, for instance using QGIS, allowing the creation of spatial probability maps of potential nesting sites.

In the future, this methodology could be complemented with other non-invasive technologies, such as thermal imaging, which may detect temperature anomalies above the nesting chamber and confirm the presence of eggs. By combining these methods, sea turtle nests can be detected with greater precision and without direct interference, thereby minimizing the risk of egg damage or

habitat disturbance. The entire experimental workflow, including the steps, tools used, and their interconnections, is illustrated in Figure 23.

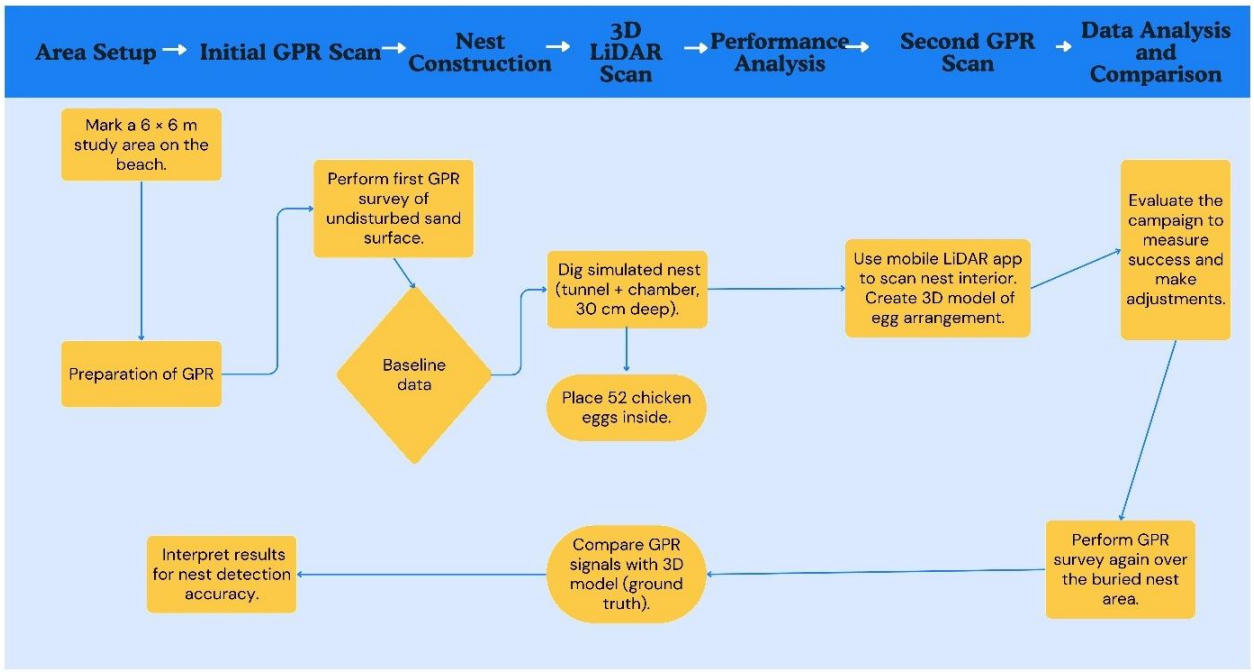

Figure 23. Experimental procedure for sea turtle nest detection. Methodology filled out the setting and delineating a test site of 6 × 6 m on the beach, GPR exploration of the beach with undisturbed sand is accomplished to have baseline reference data. After that, a nest is fabricated (a chamber with a tunnel, around 30 cm deep) made up of 52 chicken eggs representing a natural sea turtle nesting chamber. The interior of the nest structure is photographed and mapped by a mobile LiDAR system generating a 3D model. Next, a further GPR survey is made at the same place, and the outcomes are contrasted with the LiDAR-derived 3D model to measure the precision and the radar's ability to detect subsurface anomalies. Afterward, data evaluation is done to determine the efficiency of the method and to suggest possible enhancements for the next uses.

4. Results

4.1 GPR Results and Interpretation

An example of a GPR B-scan and interpolated horizontal slice (Figure 24.) obtained from data collected over a 20 × 20 cm grid is presented below. The highlighted anomaly (red box) corresponds to the reconstructed sea turtle nest, experimentally simulated using buried chicken eggs. The B-scan shows a distinct hyperbolic reflection pattern at a depth of approximately 0.34 m, while the corresponding horizontal slice reveals a localized high-amplitude response in the same area, confirming the presence of the artificial nest.

It is important to note a discrepancy between the total construction depth of the nest (52 cm) and the depth detected by the GPR (34 cm). This difference of 18 cm can be technically explained by the fact that GPR detects the upper boundary of a subsurface anomaly. In this case, the first layer of the buried egg clutch, rather than the bottom of the excavated shaft. This interpretation is further supported by the 3D LiDAR reconstruction, which provided a reference for the internal geometry of the nest. The LiDAR model confirmed that the top of the egg chamber was located at a depth of approximately 29 cm, which aligns closely with the 34 cm depth identified in the radargram.

Other smaller anomalies visible in the B-scan and horizontal slice can be attributed to natural heterogeneities within the sandy beach environment rather than buried objects. Slight variations in moisture content, grain size, or sediment compaction may locally alter the dielectric properties of the substrate, resulting in weak reflections or scattered amplitude anomalies. Shallow stratigraphic discontinuities, such as thin layering or interfaces between sands of different moisture levels, may also generate subhorizontal reflectors.

Additionally, some anomalies may have been caused by pebbles embedded beneath finer sediments, producing localized high-amplitude reflections due to pronounced dielectric contrasts. Minor artifacts may also have arisen from surface disturbances or from interpolation of the data collected over the 20 × 20 cm grid.

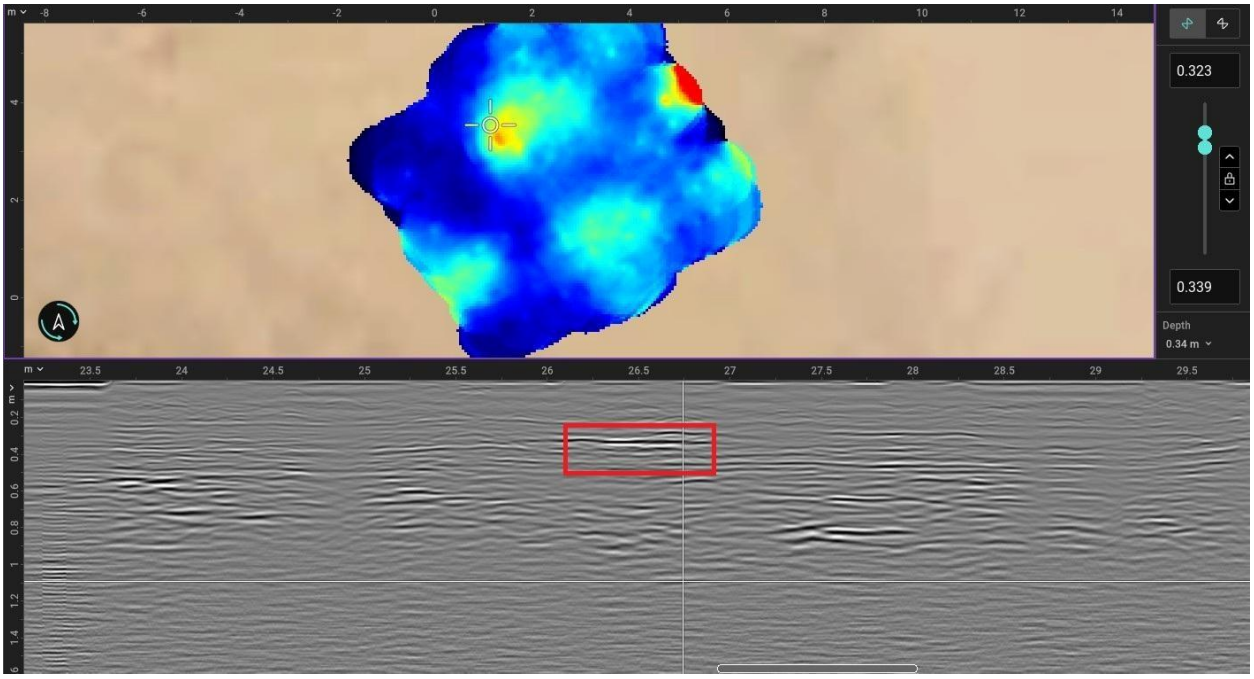

Figure 24. Result of GPR measurements in the experimental area. The lower section shows the B-scan with a distinct hyperbolic anomaly (red box), while the upper section presents the interpolated horizontal slice displaying increased amplitude at the location of the simulated sea turtle nest.

4.2 LiDAR Visualization of the Simulated Nest

LiDAR technology represents a powerful tool for precise 3D visualization of natural objects. In this study, it was used to create a detailed spatial reconstruction of the simulated sea turtle nest, allowing for the assessment of the nest chamber's shape, dimensions, and its relation to the surrounding substrate. LiDAR provides a major advantage by enabling the acquisition of highly accurate data without physically disturbing the sand or exposing the chamber, thereby preserving the integrity of the studied structure. This method thus serves as an ideal complement to geophysical GPR measurements, as it provides a reference 3D model that can be used to validate subsurface anomalies detected by radar.

Using a mobile LiDAR system, a 3D model of the simulated sea turtle nest was generated, providing a detailed visualization of the chamber and the spatial arrangement of the eggs. The reconstruction allowed for precise measurement of the chamber depth, which ranged between 29 and 52 cm. The models clearly display the tunnel-like structure of the nest, with a narrow entrance

extending into an enlarged lower section representing the egg chamber, consistent with the typical morphology of Caretta caretta nests.

The LiDAR model also enabled visual inspection of egg distribution and their positioning relative to the chamber walls, allowing for estimates of egg density and total nest cavity volume. This information was subsequently used as reference data for comparison with GPR scanning results obtained from the same area. Comparing both methods allowed for validation of radar data accuracy and improved interpretation of the detected anomalies.

Figure 25 A–H. 3D LiDAR reconstruction of the simulated sea turtle nest. The models illustrate the tunnel-shaped structure of the nesting chamber, the spatial arrangement of the eggs, and the measured depth (29–52 cm).

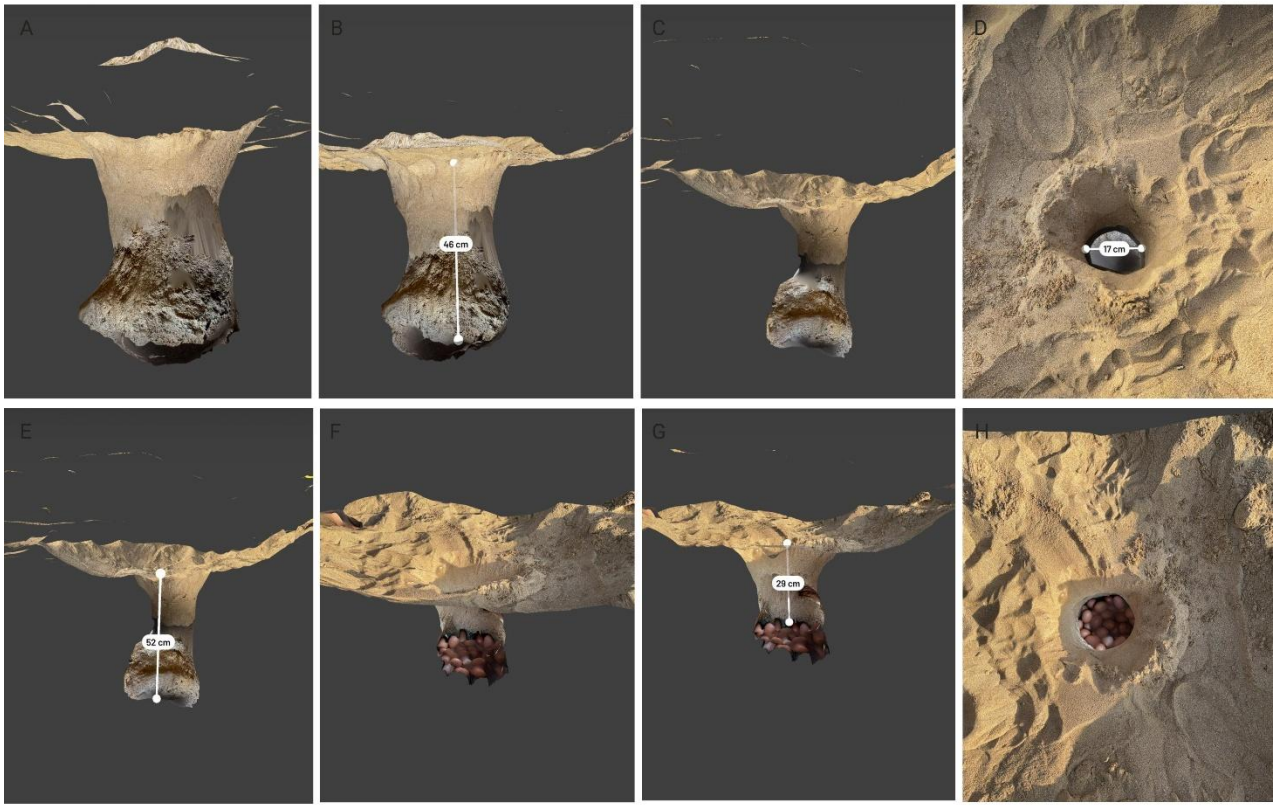

Figure 25. A–H. 3D LiDAR reconstruction of the simulated sea turtle nest. The models illustrate the tunnel-shaped structure of the nesting chamber, the spatial arrangement of the eggs, and the measured depth (29–52 cm).

4.3 AI Detection Results

The trained artificial intelligence model, based on the YOLOv8 architecture, was used to detect sea turtle tracks in the annotated photographs. The objective was to evaluate its ability to automatically recognize the characteristic patterns of loggerhead turtle (*Caretta caretta*) tracks and distinguish them from other visually similar objects, such as human footprints, rocks, or debris.

The evaluation of the model's performance was conducted in two distinct stages. First, the learning process was monitored using the validation subset of the 36 manually annotated images. Subsequently, the trained model was deployed on the remaining 118 images of the total 154 dataset. These 118 images served as an independent test set, allowing for an assessment of the model's robustness and generalization capabilities on unseen data, including various lighting conditions and aerial drone perspectives.

4.3.1 Model performance during training

In Figure 26, the training and validation curves of the loss functions and performance metrics are shown. The graphs *train/box_loss*, *train/cls_loss*, and *train/dfl_loss* indicate that all three types of losses gradually decreased, confirming that the model successfully learned to recognize objects and improved both localization and classification accuracy. A similar trend can be observed for the validation data (*val/box_loss*, *val/cls_loss*, *val/dfl_loss*), which demonstrates consistent learning without significant overfitting. The curves of precision, recall, and mean Average Precision (mAP) show an upward trend that gradually stabilizes over the course of the epochs. The training and validation patterns are very similar, suggesting mild but expected overfitting due to the small number of training images (36).

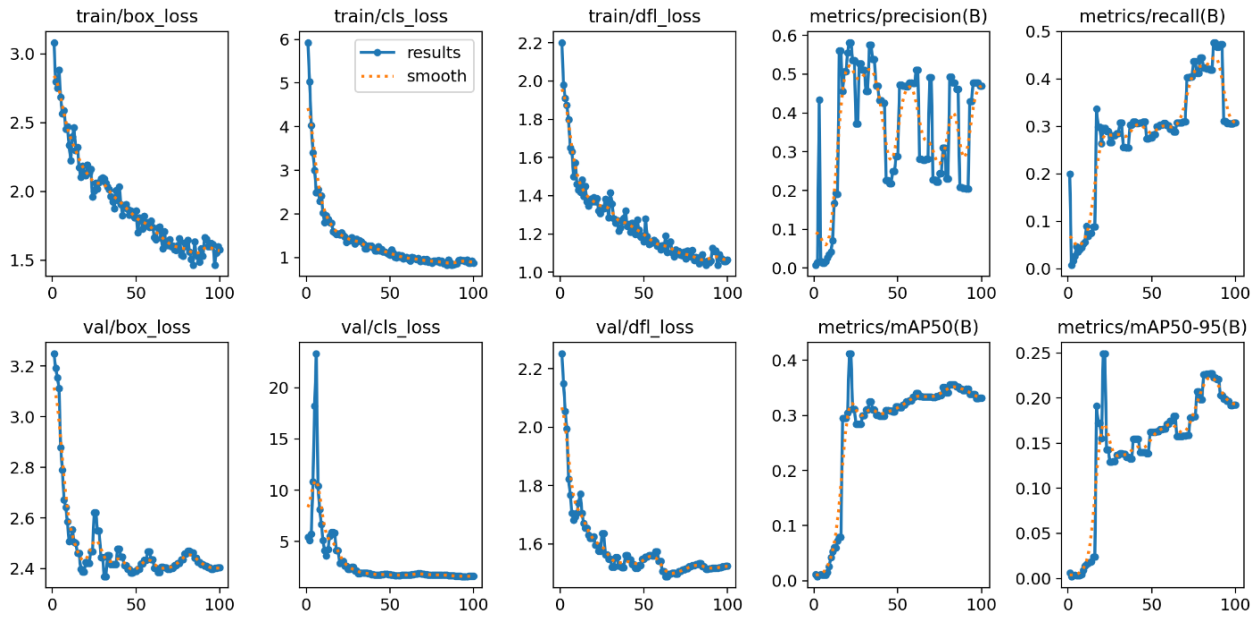

Figure 26. Training performance of the YOLOv8 model. The figures report the changes of the main loss functions, box, classification, and distribution focal loss (DFL), for the training and validation datasets, along with the performance metrics (precision, recall, and mean Average Precision at IoU thresholds of 0.5 and 0.5, 0.95) obtained. The gradual reduction of all losses and the corresponding increment of precision and mAP demonstrate that the model has learned effectively and has converged during training.

4.3.2 Data and class distribution

The distribution of annotated objects in the training dataset shows a pronounced class imbalance (Figure 28). The class *turtle_tracks* constitutes the dominant portion of all annotations, while the remaining classes (e.g., *people*, *boats*, *bins*, *rocks*) are represented only minimally. This imbalance is reflected in the model's behavior, which achieved its best performance for the turtle track class.

The bounding box position distribution graphs indicate that most annotated objects are located in the central part of the images and are relatively small in size, corresponding to the typical scale of turtle tracks in the photographs.

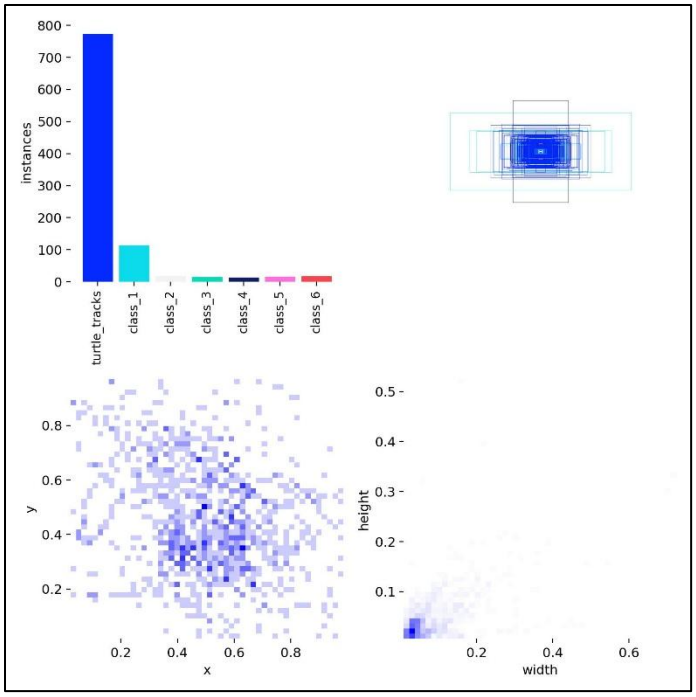

Figure 27. Distribution of annotated objects within the training dataset. The bar chart shows the number of labelled objects per class, illustrating a strong imbalance between categories, with the class turtle_tracks dominating the dataset. The accompanying spatial distribution maps indicate that most bounding boxes are concentrated near the centre of the images and are relatively small in size, reflecting the typical scale and position of turtle track annotations.

4.3.3 Model results and performance evaluation

The Precision-Confidence Curve (Figure 29.) shows that prediction precision increases with a higher confidence threshold. At high confidence levels, the model achieves high precision (~0.9), indicating that when the model is confident in its predictions, the occurrence of false-positive detections is very low.

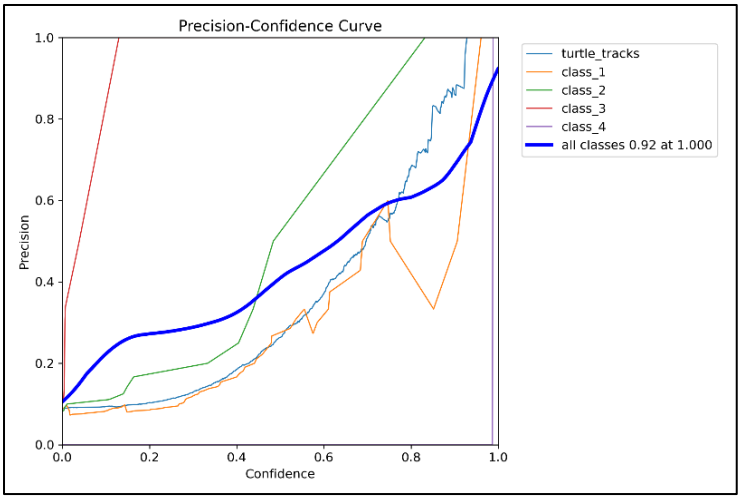

Figure 28. Precision-Confidence curve for the YOLOv8 model.

Figure 28. illustrates the relationship between prediction precision and the confidence threshold. Precision increases steadily with higher confidence values, reaching up to approximately 0.9 at high thresholds, indicating that the model produces very few false-positive detections when predictions are made with high certainty.

On the other hand, the Recall-Confidence Curve (Figure 29.) demonstrates the opposite trend-high recall values are achieved at low confidence thresholds (the model detects most objects but with a higher number of false detections), while recall decreases as the confidence level increases. The Precision-Recall (PR) Curve (Figure 30.) illustrates the typical trade-off between these two metrics and confirms that the model performs best for the *turtle_tracks* class, with a mean Average Precision (mAP@0.5) of approximately 0.41.

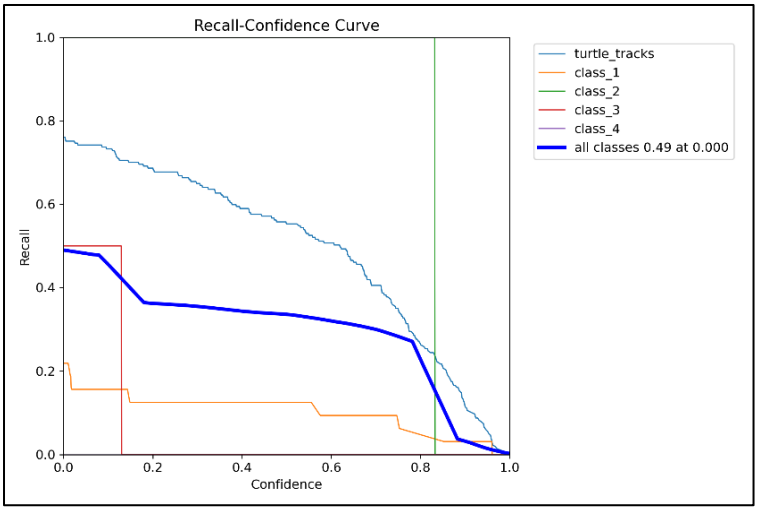

Figure 29. Recall-Confidence curve for the YOLOv8 model.

Figure 29. demonstrates the inverse relationship between recall and the confidence threshold: recall values are high at low confidence levels, indicating that the model successfully detects most objects, but gradually decreases as the confidence threshold increases. This trend reflects the typical trade-off between sensitivity and precision in object detection models.

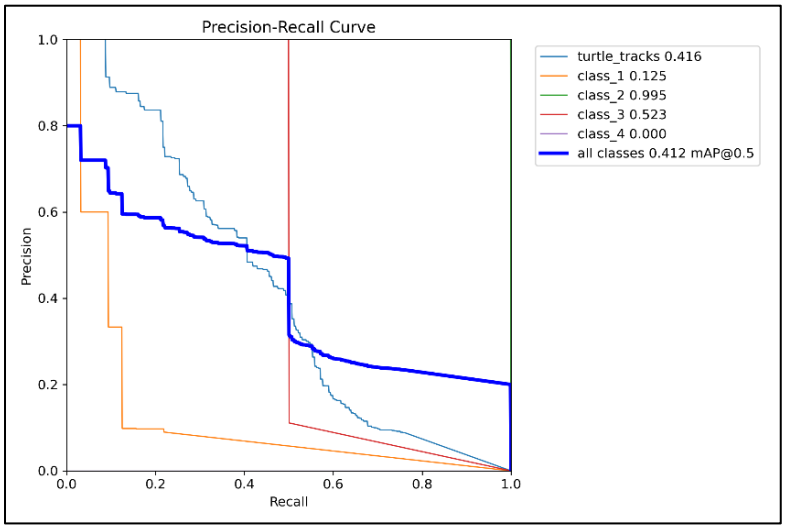

Figure 30. Precision-Recall (PR) curve for all object classes in the YOLOv8 model.

Figure 30. illustrates the typical trade-off between precision and recall, with each curve representing one annotated class. The model achieves its best performance for the turtle_tracks

class, with a mean Average Precision (mAP@0.5) of approximately 0.41, confirming the dominance of this class in the training dataset.

Overall, the model demonstrates high precision at higher confidence thresholds and a moderate level of recall, meaning that it reliably confirms true tracks but may overlook some less distinct or partially obscured ones. This outcome is entirely expected given the limited amount of training data and the variability of the input images (different lighting conditions, viewing angles, and substrate types).

4.3.4 Qualitative comparison: predictions vs. annotations

The comparison between manually annotated and model-predicted images (Figures F and G) shows that the model successfully detected most of the tracks in the test images, including those captured by drones from higher altitudes. The model correctly outlined the main track areas and assigned them high confidence scores. In a few cases, false-positive detections appeared in areas containing human footprints or tyre marks, particularly in photographs with lower contrast (e.g., taken at sunset or under red light).

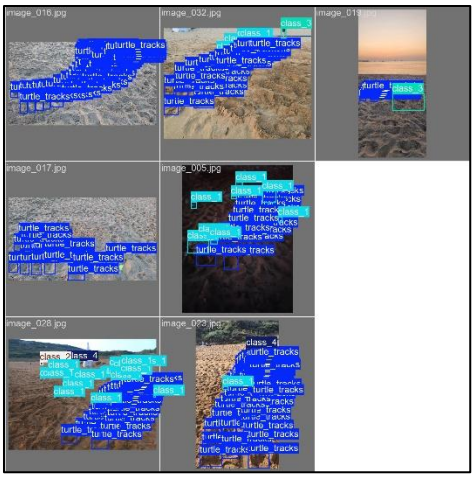

Figure 31. Ground-truth bounding boxes defined during the annotation process using MakeSense.ai.

The Figure 31. shows manually labelled classes, including turtle tracks and other surface elements, which served as reference data (validation labels) for training and model evaluation.

Figure 32. The trained YOLOv8 model predicted bounding boxes (validation predictions).

Figure 32. demonstrates successful detection of turtle tracks on both ground-based and aerial drone photographs. High-confidence detections correspond closely to the annotated regions, while occasional false positives appear in areas with footprints or tyre marks.

The trained YOLOv8 model confirmed its ability to recognize sea turtle tracks across different types of images. Despite the limited amount of training data, it achieved a good level of accuracy and robustness, demonstrating the potential of AI as an effective tool for automated monitoring of nesting beaches. The results also confirm that expanding the training dataset, balancing the classes, and optimizing the network architecture (e.g., adjusting YOLOv8 parameters or applying transfer learning) could significantly improve detection performance in real-world applications.

This approach represents an important step toward developing a fully automated system for monitoring turtle track occurrences, which could, in the future, be integrated with other non-invasive technologies (LiDAR, GPR) and applied in conservation practice.

5. Discussion

The objective of this study was to explore the potential of combining non-invasive technologies, Ground Penetrating Radar (GPR), Artificial Intelligence (AI), and LiDAR scanning, for the detection and monitoring of sea turtle nests. Although the experimental work was based on a simulated nest rather than real turtle clutches, the results and observations obtained during the field procedures provide valuable insights into the feasibility, limitations, and practical implications of these techniques within a conservation context.

5.1 Ground Penetrating Radar (GPR) performance

The GPR method demonstrated strong potential for detecting subsurface anomalies corresponding to the structure of a turtle nest. The experiment showed that the technique can distinguish variations in sand compaction and moisture, which are among the most critical parameters influencing radar signal quality. A key observation in this context was the 18 cm discrepancy between the physical nest depth (52 cm) and the GPR detection depth (34 cm). This difference is a known characteristic of GPR technology, which typically identifies the upper boundary of an anomaly. In this case, the top of the egg clutch, rather than the maximum depth of the excavation. This interpretation is validated by the LiDAR data, which placed the top of the chamber at 29 cm, confirming that the radar successfully localized the most significant dielectric contrast. For future applications, this depth variance must be factored into interpretation protocols to avoid underestimating the actual nesting depth. The visibility of the simulated egg chamber depended largely on the contrast between the surrounding sand and the material within the cavity. In general, dry and homogeneous sand conditions, such as those found at Golden Bay during the experiment, are favorable for radar penetration and reflection clarity. However, in natural settings, variations in moisture, grain size, or the presence of organic material may complicate signal interpretation. These observations confirm findings from previous ecological studies suggesting that while GPR is a powerful tool, it requires site-specific calibration and careful data processing to avoid false positives or misinterpretation.

Regarding the experimental setup, chicken eggs were used as a functional proxy for sea turtle eggs due to their similar fluid-filled structure, which creates a significant dielectric contrast against dry sand (Ermakov et al., 2012). While sea turtle eggs have more leathery shells compared to the calcified shells of chicken eggs, the primary factor for GPR detection is the high permittivity of the internal egg content relative to the surrounding substrate. As demonstrated by Ermakov et al. (2012), although turtle nest detection is challenging due to environmental noise, the dielectric contrast between the buried biological objects and the soil remains the fundamental principle for successful localization.

Additionally, while measurements on undisturbed sand were conducted as a baseline (Figure 23), their role was primarily to calibrate the background signal and confirm the absence of natural subsurface anomalies. This ensured that the subsequent reflections observed in the data were uniquely attributable to the presence of the simulated nest, providing a necessary reference for the identification of the target anomaly.

Furthermore, it is essential to acknowledge the structural and environmental differences between the simulated nest used in this study and natural sea turtle nests. A natural nest is characterized by a specific humidity gradient and gas exchange environment created by the metabolic heat of developing embryos, which can alter the dielectric properties of the surrounding sand over time (Najwa-Sawawi et al., 2021). Natural nesting sites also often contain organic debris, roots, or varying layers of shell fragments that increase 'background noise' in GPR data. While this feasibility study successfully localized a controlled anomaly, the interpretability of results in a natural setting may be affected by these environmental complexities Furthermore, it is essential to acknowledge the structural and environmental differences between the simulated nest used in this study and natural sea turtle nests. A natural nest is characterized by a specific humidity gradient and gas exchange environment created by the metabolic heat of developing embryos, which can alter the dielectric properties of the surrounding sand over time (Najwa-Sawawi et al., 2021). Natural nesting sites also often contain organic debris, roots, or varying layers of shell fragments that increase 'background noise' in GPR data. While this feasibility study successfully localized a controlled anomaly, the interpretability of results in a natural setting may be affected by these environmental complexities. Future research should therefore focus on testing these non-invasive tools on natural nests to account for the dynamic biological and physical variables inherent in wild

nesting habitats (Najwa-Sawawi et al., 2021). Future research should therefore focus on testing these non-invasive tools on natural nests to account for the dynamic biological and physical variables inherent in wild nesting habitats.

In addition, it is important to address the absence of quantitative statistical metrics, such as false positive (FP) and false negative (FN) rates, in this evaluation. Since this study was designed as a feasibility case study with a single confirmed nest (n=1) and did not include independent, ground-truthed negative controls (verified areas where absence of a nest is confirmed), calculating FP/FN rates would be statistically meaningless and not generalisable. Additionally, GPR traces and time-slice cells cannot be treated as independent trials due to their strong spatial and temporal correlation. Treating them as such would artificially inflate the sample size and yield misleading precision.

Consequently, this research focuses on indicators appropriate for the available data: detection outcome, localisation and geometry consistency against the LiDAR reference, and anomaly interpretability. Future work requiring replicated trials across multiple nests, verified negatives, and varying field conditions (e.g., moisture and sediment properties) will be necessary to establish robust statistical performance rates.

5.2 3D LiDAR reconstruction as validation tool

The LiDAR-based 3D reconstruction of the simulated nest provided an effective visual reference for validating radargrams and understanding the internal geometry of the cavity. This approach enabled a comparison between the actual structure and the patterns visible in radar data, contributing to a more accurate interpretation of GPR results. Although the LiDAR scan was conducted manually and thus contained minor inaccuracies, it proved valuable for illustrating how 3D documentation can complement geophysical data. Such visual models can also serve as educational or communication tools in conservation and research, facilitating better understanding of the nesting environment without the need for excavation.

5.3 AI-based track detection

The application of artificial intelligence (AI) for sea turtle track detection proved to be a promising step toward automating one of the most time-consuming aspects of nesting beach monitoring. The model, based on convolutional neural networks (CNNs) and trained on datasets provided by the University of Cádiz and Nature Trust Malta, successfully recognized the characteristic linear and curved patterns created by female loggerhead turtles (*Caretta caretta*) as they move across the beach. This confirmed that neural networks can effectively identify biological traces under natural conditions and thus significantly improve the efficiency of fieldwork (Zhao et al., 2019; Zou et al., 2023). The overall performance of the model was highly satisfactory given the limited number of training images (n = 36), exceeding expectations for a quickly implemented test version.

Despite these positive results, several limitations were identified that affected detection accuracy and reliability. The most significant issue was the heterogeneity of the input data. Images from different sources varied in resolution, viewing angle, and lighting conditions. In particular, photographs taken during night patrols under red light exhibited lower contrast, making track recognition more difficult. In some cases, turtle tracks were misclassified as tyre marks, human footprints, or shadows of washed-up debris.

Another factor influencing the results was the architecture of the YOLOv8 (*You Only Look Once*) model. Although this latest version significantly improves upon the original limitations described by Redmon et al. (2016), some structural constraints remain, particularly when detecting overlapping or elongated objects. This can reduce localization accuracy in situations where individual tracks intersect or occur in close proximity. The network also tends to lose fine details due to repeated downsampling, which makes it difficult to capture small or narrow structures. Even a minor localization deviation can substantially affect the Intersection over Union (IoU) metric, leading to a higher number of false-negative detections (Redmon et al., 2016).

The model was further affected by the natural variability of the tracks themselves. The appearance of loggerhead turtle tracks changes depending on sand moisture, beach slope, and the individual behaviour of females. Consequently, the dataset contained both deeply imprinted and shallow or partially disturbed tracks. In several instances, the model interpreted incomplete imprints as

background, highlighting the need for further expansion and balancing of the training dataset (Zhao et al., 2019).

Despite these limitations, integrating AI with LiDAR and GPR technologies has proven to be highly beneficial. The AI model was able to pre-identify probable track areas, thereby reducing the spatial extent required for subsequent geophysical surveys. This approach not only shortened field survey time but also minimized human disturbance in sensitive nesting habitats. The inclusion of additional annotated categories (e.g., rocks, vegetation, debris) further enhanced the model's ability to distinguish natural from anthropogenic features, reducing the number of false detections (Zou et al., 2023).

Future efforts should focus on expanding and diversifying the training data, including images captured under different lighting conditions and substrate types. It would also be valuable to test more advanced neural network architectures, such as YOLOv9 or Faster R-CNN, which achieve superior results in small-object detection and enable more precise localization (Zhao et al., 2019; Zou et al., 2023). Another promising direction could involve the use of *transfer learning* - transferring knowledge from related tasks (e.g., detection of tracks from other animal species) - which could shorten training time and improve accuracy in cases with limited data availability.

The overall performance of the YOLOv8 model was highly satisfactory, especially considering the limited training set of 36 manually annotated images. The successful generalization of the model when applied to the independent test set of 118 unseen images confirms its robustness. Even though the training and validation curves indicated a mild degree of overfitting, which is expected with a smaller training dataset, the model's ability to accurately identify tracks in diverse lighting and different drone perspectives demonstrates its practical utility for real-world beach monitoring. Ultimately, AI-based track detection represents an effective, non-invasive, and scalable tool for supporting sea turtle conservation. While accuracy remains influenced by data quality, continuous dataset expansion and integration with complementary methods (LiDAR, GPR) promise further increases in reliability and practical applicability (Redmon et al., 2016; Zhao et al., 2019; Zou et al., 2023).

5.4 Integration of methods and conservation implications

It is one of the main results of this work, in fact, the proof that the coupling of complementing non, invasive techniques can increase precision and the confidence of the detection of nests while the safety of the turtles as well as the safety of the habitats is a least of all disturbances. Every procedure has its own advantages, GPR for below, ground situations, LiDAR for the visualization of structures, and AI for the recognition of patterns on the surface, and on their own they are a multi-level strategy which can be used in real conservation scenarios.

While Section 4 presents the results of each technology independently, their integration lies in a sequential workflow that reduces uncertainty. The AI-based recognition serves as a wide-area screening tool to identify high-probability zones, GPR provides subsurface verification, and LiDAR confirms the precise geometry of the nesting chamber. Although a quantitative statistical correlation between these methods was not feasible in this feasibility study (n=1), their qualitative synergy significantly increases the reliability of nest detection compared to using a single method alone.

In tiny nesting areas like Malta, where such events are infrequent, and the human presence on the beaches are high, these approaches might provide a beneficial solution to the invasive methods that is currently being used. Further experiments under natural nesting conditions are still required, but the methods here put forward are an initial step to future research directions.

The instruments here are also a steppingstone to the eventual goal of the creation of novel, tech, led conservation strategies which feature the symbiosis of ecological and technological knowledge in data collection and analysis.

Implementing this integrated technological approach in real-world conservation involves specific practical considerations. In terms of cost, the use of mobile-based LiDAR and AI offers a significant advantage, as it utilizes existing consumer hardware (e.g., iPhone Pro models), avoiding the need for expensive industrial scanners. The primary cost for GPR remains the initial equipment acquisition or professional service hiring, though its long-term use reduces the expenses associated with manual excavation and potential nest damage. Regarding time requirements, while AI screening can process large datasets from drone surveys in minutes, the in-situ application of GPR

and LiDAR is more demanding. Depending on environmental conditions and the necessary site preparation (including equipment setup and calibration), the process typically requires at least 60 to 90 minutes per potential nesting site to ensure high-quality data collection. Furthermore, while AI and LiDAR tools are increasingly user-friendly, the interpretation of GPR radargrams still requires specialized training or collaboration with geophysicists. Therefore, a successful implementation would benefit from a multi-disciplinary team where park rangers handle data collection while specialists provide the final data verification.

In continuation of this project, a 25-minute documentary was produced which captures the field activities, such as GPR surveying and the 3D LiDAR reconstruction of the artificially created nest. While the documentary was produced as an independent outreach initiative, its inclusion here provides a visual record of the methodologies described in this thesis. By capturing the real-time application of these tools on the beach, the film demonstrates the practical execution of the field workflow, offering a perspective on the site conditions that complements the technical descriptions in the methodology sections. Consequently, the video serves to enhance the transparency of the experimental procedures and aids in communicating the practical potential of these non-invasive tools to a non-technical audience (Fürychová, 2025).

6. Conclusion

This study explored the potential of non-invasive technologies for detecting and monitoring sea turtle nests, focusing on the combined application and evaluation of Ground Penetrating Radar (GPR), Artificial Intelligence (AI), and 3D LiDAR scanning. The primary aim was to test and assess this combination of techniques to evaluate whether they can provide accurate and efficient conservation efforts while minimizing disturbance to nesting turtles and their natural habitats.

The experiment conducted on a simulated loggerhead turtle (*Caretta caretta*) nest at Golden Bay met the research objectives by demonstrating that GPR can identify subsurface anomalies resembling the geometry of a real nest. However, the accuracy of detection is strongly influenced by the physical characteristics of the sand, such as moisture content and grain size. LiDAR proved to be an effective tool for 3D visualization and for validating radar data, while AI showed promising potential for automating the recognition of turtle tracks and early identification of nesting events.

The integration of these techniques represents an innovative and sustainable framework for sea turtle research and conservation. Their combined use can enhance the efficiency of monitoring programs, improve nest localization accuracy, and reduce human interference during critical reproductive stages. By linking these technological findings to the initial research objectives, this study provides a foundational workflow for non-invasive monitoring.

Although the present research provides proof of concept, further studies are required to refine and validate these techniques under real nesting conditions. Future work should involve field testing on natural nests, carried out in collaboration with authorized conservation organizations such as Nature Trust Malta, to ensure ethical and legal compliance.

The optimization of GPR signal interpretation under varying sand conditions through calibration protocols, and the integration of machine learning into radar data processing, could significantly improve the accuracy of subsurface detection. Similarly, expanding the AI training dataset to include a greater variety of environmental and lighting conditions would increase model reliability.

Another promising direction is the development of an integrated monitoring platform that combines GPR data, AI-based surface detection, and 3D mapping into a single workflow.

Applying these methods across different Mediterranean beaches would enable comparative studies and contribute to broader regional conservation strategies. Ultimately, interdisciplinary collaboration between ecologists, geophysicists, and computer scientists will be essential to fully realize the potential of technological innovation in sea turtle conservation.

References

Aber, J. S., Marzolff, I., & Ries, J. B. (2010). Small-format aerial photography: Principles, techniques and geoscience applications. Elsevier Science.

Ackerman, R. A. (1997, January 1). The Nest Environment And The Embryonic Development Of Sea Turtles. https://www.researchgate.net/publication/265270095_The_Nest_Environment_And_The_Embryonic_Development_Of_Sea_Turtles

Alessandro, L., & Antonello, S. (2010). An overview of loggerhead sea turtle (Caretta caretta) bycatch and technical mitigation measures in the Mediterranean Sea. Reviews in Fish Biology and Fisheries, 20(2), 141–161. https://doi.org/10.1007/s11160-009-9126-1

Annan, A. P. (2002). GPR—History, Trends, and Future Developments. Subsurface Sensing Technologies and Applications, 3(4), 253–270. https://doi.org/10.1023/A:1020657129590

Annan, A. P. (2009). Electromagnetic Principles of Ground Penetrating Radar. In Ground Penetrating Radar Theory and Applications (pp. 1–40). Elsevier. https://doi.org/10.1016/B978-0-444-53348-7.00001-6

Annan, A. P. (2009). Electromagnetic Principles of Ground Penetrating Radar. In Ground Penetrating Radar Theory and Applications (pp. 1–40). Elsevier. https://doi.org/10.1016/B978-0-444-53348-7.00001-6

B., W. (2002). Ecology of neonate loggerhead turtles inhabiting lines of downwelling near a Gulf Stream front. Marine Biology, 140(4), 843–853. https://doi.org/10.1007/s00227-001-0737-x

Baker, G. S., Jordan, T. E., & Pardy, J. (2007). An introduction to ground penetrating radar (GPR). In Special Paper 432: Stratigraphic Analyses Using GPR (Vol. 432, pp. 1–18). Geological Society of America. https://doi.org/10.1130/2007.2432(01)

Bjorndal, K. A. (1980). Nutrition and grazing behavior of the green turtle Chelonia mydas. Marine Biology, 56(2), 147–154. https://doi.org/10.1007/BF00397131

Bjorndal, K. A., Bolten, A. B., & Chaloupka, M. Y. (2000). GREEN TURTLE SOMATIC GROWTH MODEL: EVIDENCE FOR DENSITY DEPENDENCE. Ecological Applications, 10(1), 269–282. https://doi.org/10.1890/1051-0761(2000)010%255B0269:GTSGME%255D2.0.CO;2

Bolten, A. B., & Witherington, B. E. (2003). Loggerhead sea turtles. Smithsonian books.

Bouchard, S. S., & Bjorndal, K. A. (2000). SEA TURTLES AS BIOLOGICAL TRANSPORTERS OF NUTRIENTS AND ENERGY FROM MARINE TO TERRESTRIAL ECOSYSTEMS. Ecology, 81(8), 2305–2313. https://doi.org/10.1890/0012-9658(2000)081%255B2305:STABTO%255D2.0.CO;2

Bowen, B. W., & Karl, S. A. (2007). Population genetics and phylogeography of sea turtles. Molecular Ecology, 16(23), 4886–4907. https://doi.org/10.1111/j.1365-294X.2007.03542.x

Bristow, C. S., & Jol, H. M. (2003). An introduction to ground penetrating radar (GPR) in sediments. Geological Society, London, Special Publications, 211(1), 1–7. https://doi.org/10.1144/GSL.SP.2001.211.01.01

Casale, P., & Margaritoulis, D. (2010). Sea turtles of the Mediterranean: Distribution, threats and conservation priorities. International Union for Conservation of Nature and Natural Resources.

Casale, P., Broderick, A., Camiñas, J., Cardona, L., Carreras, C., Demetropoulos, A., Fuller, W., Godley, B., Hochscheid, S., Kaska, Y., Lazar, B., Margaritoulis, D., Panagopoulou, A., Rees, A., Tomás, J., & Türkozan, O. (2018). Mediterranean sea turtles: Current knowledge and priorities for conservation and research. Endangered Species Research, 36, 229–267. https://doi.org/10.3354/esr00901

CITES Convention on International Trade in Endangered Species of Wild Fauna and Flora. Appendices I, II and III. Available online: https://cites.org/sites/default/files/eng/app/2023/E-Appendices-2023-05-21.pdf (accessed on 1 November 2025).

CloudCompare (version 2.13.2) [Computer software]. (2024). Retrieved from http://www.cloudcompare.org/

Colica, E. (2022). Geophysics and geomatics methods for coastal monitoring and hazard evaluation. https://www.um.edu.mt/library/oar/bitstream/123456789/106954/1/PhD_Thesis_Emanuele_Colica.pdf

Dalal, N., & Triggs, B. (2005). Histograms of Oriented Gradients for Human Detection. 2005 IEEE Computer Society Conference on Computer Vision and Pattern Recognition (CVPR'05), 1, 886–893. https://doi.org/10.1109/CVPR.2005.177

Dong, Y., & Ansari, F. (2011). Ground-Penetrating Radar - an overview | ScienceDirect Topics. Sciencedirect.com. https://www.sciencedirect.com/topics/materials-science/ground-penetrating-radar

Dutton, D. L., Dutton, P. H., Chaloupka, M., & Boulon, R. H. (2005). Increase of a Caribbean leatherback turtle Dermochelys coriacea nesting population linked to long-term nest protection. Biological Conservation, 126(2), 186–194. https://doi.org/10.1016/j.biocon.2005.05.013

Eckert, K. L. (1999). Research and management techniques for the conservation of sea turtles. IUCN/SSC Marine Turtle Specialist Group.

Ermakov, V., Dubrawski, A., Hodgins, J., Dohi, T., & Savage, A. (2012). Mining sea turtle nests: An amplitude independent feature extraction method for GPR data. 2012 14th International Conference on Ground Penetrating Radar (GPR), 393–398. https://doi.org/10.1109/ICGPR.2012.6254897

Felzenszwalb, P., McAllester, D., & Ramanan, D. (2008). A discriminatively trained, multiscale, deformable part model. 2008 IEEE Conference on Computer Vision and Pattern Recognition, 1–8. https://doi.org/10.1109/CVPR.2008.4587597

Fürychová, B. (2025). The Edge of Survival. YouTube. https://www.youtube.com/channel/UCE-JKK64c0kMzi-fyHyyU2A

GFCM Recommendation GFCM/35/2011/4 on the Incidental Bycatch of Sea Turtles in Fisheries in the GFCM Area of Application. 2011. Available online: https://faolex.fao.org/docs/pdf/mul201486.pdf (accessed on 1 November 2025).

H. El-said, M. (1956). Geophysical Prospection of Underground Water in the Desert by Means of Electromagnetic Interference Fringes. Proceedings of the IRE, 44(1), 24–30. https://doi.org/10.1109/JRPROC.1956.274846

Hawkes, L. A., Broderick, A. C., Godfrey, M. H., & Godley, B. J. (2007). Investigating the potential impacts of climate change on a marine turtle population. Global Change Biology, 13(5), 923–932. https://doi.org/10.1111/j.1365-2486.2007.01320.x

Hays, G. C. (2005). Stemming the tide of turtle extinction. Nature, 433(7022), 109–109. https://doi.org/10.1038/433109a

Hirth, H. F. (1971). SYNOPSIS OF BIOLOGICAL DATA ON IHE GREEN TUTLE Chelonia mydas (Linnaeus) 1758 Prepared by ftF. Hirth FOOD AND AGRICULTURE OGANIZATION OF THE UNITED NATIONS. https://www.fao.org/4/c3466e/c3466e.pdf

ICCAT Recommendation by ICCAT Amending Recommendation 10-09 on the By-Catch of Sea Turtles in ICCAT Fisheries. 2011. Available online: https://www.iccat.int/Documents/Recs/compendiopdf-e/2013-11-e.pdf (accessed on 1 November 2025).

in. (2015, March 19). Physics Stack Exchange. Physics Stack Exchange. https://physics.stackexchange.com/questions/171144/do-electromagnetic-waves-occupy-varying-amounts-of-space-or-do-they-simply-vary

IUCN. (2025). The IUCN Red List of Threatened Species. IUCN Red List; International Union for Conservation of Nature and Natural Resources. https://www.iucnredlist.org/

Kruk, J. V. D., Wapenaar, C. P. A., Fokkema, J. T., & Van Den Berg, P. M. (2003). Three-dimensional imaging of multicomponent ground-penetrating radar data. GEOPHYSICS, 68(4), 1241–1254. https://doi.org/10.1190/1.1598116

Lee, P. L. M., Luschi, P., & Hays, G. C. (2007). Detecting female precise natal philopatry in green turtles using assignment methods. Molecular Ecology, 16(1), 61–74. https://doi.org/10.1111/j.1365-294X.2006.03115.x

Lewison, R. L., Freeman, S. A., & Crowder, L. B. (2004). Quantifying the effects of fisheries on threatened species: The impact of pelagic longlines on loggerhead and leatherback sea turtles. Ecology Letters, 7(3), 221–231. https://doi.org/10.1111/j.1461-0248.2004.00573.x

Lohmann, K. J., Salmon, M., & Wyneken, J. (1990). Functional Autonomy of Land and Sea Orientation Systems in Sea Turtle Hatchlings. The Biological Bulletin, 179(2), 214–218. https://doi.org/10.2307/1541772

Micheli, F., Halpern, B. S., Walbridge, S., Ciriaco, S., Ferretti, F., Fraschetti, S., Lewison, R., Nykjaer, L., & Rosenberg, A. A. (2013). Cumulative Human Impacts on Mediterranean and Black Sea Marine Ecosystems: Assessing Current Pressures and Opportunities. PLoS ONE, 8(12), e79889. https://doi.org/10.1371/journal.pone.0079889

Mišijovský, J. (2013). Fotogrammetrický přístup při sběru geodat pomocí bezpilotních leteckých zařízení – Autoreferát disertační práce RNDr. Jakuba Mišijovského: Photogrammetric approach to collecting geodata using unmanned aerial vehicles. https://www.geoinformatics.upol.cz/dprace/phd/mirijovsky.pdf

Mrosovsky, N., Hopkins-Murphy, S. R., & Richardson, J. I. (1984). Sex Ratio of Sea Turtles: Seasonal Changes. Science, 225(4663), 739–741. https://doi.org/10.1126/science.225.4663.739

Nature Trust - FEE Malta. (n.d.). Nature Trust - FEE Malta. https://naturetrustmalta.org/

Najwa-Sawawi, S., Azman, N. M., Rusli, M. U., Ahmad, A., Fahmi-Ahmad, M., & Fadzly, N. (2021). How deep is deep enough? Analysis of sea turtle eggs nest relocation procedure at Chagar Hutang Turtle Sanctuary. *Saudi Journal of Biological Sciences*, *28*(9). https://doi.org/10.1016/j.sjbs.2021.05.021

Neal, A. (2004). Ground-penetrating radar and its use in sedimentology: Principles, problems and progress. Earth-Science Reviews, 66(3–4), 261–330. https://doi.org/10.1016/j.earscirev.2004.01.004

Nelms, S. E., Duncan, E. M., Broderick, A. C., Galloway, T. S., Godfrey, M. H., Hamann, M., Lindeque, P. K., & Godley, B. J. (2016). Plastic and marine turtles: A review and call for research. ICES Journal of Marine Science: Journal Du Conseil, 73(2), 165–181. https://doi.org/10.1093/icesjms/fsv165

Patel, E., Kotera, M. M., & Phillott, A. D. (2022). The roles of sea turtles in ecosystem processes and services. ResearchGate, 36. https://www.researchgate.net/publication/363862278_The_roles_of_sea_turtles_in_ecosystem_processes_and_services

Pavelka, K. (2003). Photogrammetry 10 (2nd ed.). Prague: Czech Technical University. ISBN 80-01-02649-3.

Pfaller, J. B., Bjorndal, K. A., Reich, K. J., Williams, K. L., & Frick, M. G. (2008). Distribution patterns of epibionts on the carapace of loggerhead turtles, Caretta caretta. Marine Biodiversity Records, 1, e36. https://doi.org/10.1017/S1755267206003812

Prampolini, M., Foglini, F., Biolchi, S., Devoto, S., Angelini, S., & Soldati, M. (2017). Geomorphological mapping of terrestrial and marine areas, northern Malta and Comino (central Mediterranean Sea). Journal of Maps, 13(2), 457–469. https://doi.org/10.1080/17445647.2017.1327507

Rossi, S., Mariacristina Prampolini, Galea, C., Valle, G. D., Caruana, A., & Soldati, M. (2025). Geomorphological evidence of the Malta-Sicily land-bridge during the Last Glacial Maximum inferred from seismic profiles. Earth Surface Processes and Landforms, 50(2). https://doi.org/10.1002/esp.6061

Redmon, J., Divvala, S., Girshick, R., & Farhadi, A. (2016). You Only Look Once: Unified, Real-Time Object Detection. 2016 IEEE Conference on Computer Vision and Pattern Recognition (CVPR), 779–788. https://doi.org/10.1109/CVPR.2016.91

Robinson, N. J., & Paladino, F. V. (2013). Sea Turtles. In Reference Module in Earth Systems and Environmental Sciences (p. B9780124095489043529). Elsevier. https://doi.org/10.1016/B978-0-12-409548-9.04352-9

Sella, K. A. N., Ware, M., Ceriani, S. A., Desjardin, N., Eastman, S., Addison, D., Kraus, M., Trindell, R., & Fuentes, M. M. P. B. (2023). Urban pocket beaches as nesting habitat for marine turtles: Their importance and risk from inundation. Global Ecology and Conservation, 41, e02366. https://doi.org/10.1016/j.gecco.2023.e02366

Shan, J., & Toth, C. K. (2008). Topographic Laser Ranging and Scanning. In CRC Press eBooks. Informa. https://doi.org/10.1201/9781420051438

Spotila, J. R. (Ed.). (2004). Sea turtles: A complete guide to their biology, behavior, and conservation. Johns Hopkins University Press.

Spotila, J. R. (Ed.). (2004). Sea turtles: A complete guide to their biology, behavior, and conservation. Johns Hopkins University Press.

Storelli, M. M., & Marcotrigiano, G. O. (2003). Heavy metal residues in tissues of marine turtles. Marine Pollution Bulletin, 46(4), 397–400. https://doi.org/10.1016/S0025-326X(02)00230-8

Tammina, S. (2019). Transfer learning using VGG-16 with Deep Convolutional Neural Network for Classifying Images. International Journal of Scientific and Research Publications (IJSRP), 9(10), p9420. https://doi.org/10.29322/IJSRP.9.10.2019.p9420

Troëng, S., Harrison, E., Evans, D., Haro, A. D., & Vargas, E. (2007). Leatherback Turtle Nesting Trends and Threats at Tortuguero, Costa Rica. Chelonian Conservation and Biology, 6(1), 117–122. https://doi.org/10.2744/1071-8443(2007)6%255B117:LTNTAT%255D2.0.CO;2

UNEP. (n.d.). Barcelona Convention and Protocols | UNEPMAP. Www.unep.org. https://www.unep.org/unepmap/who-we-are/barcelona-convention-and-protocols

Vella, A., & Vella, N. (2023). Conservation Genetics of the Loggerhead Sea Turtle, Caretta caretta, from the Central Mediterranean: An Insight into the Species' Reproductive Behaviour in Maltese Waters. Animals, 14(1), 137. https://doi.org/10.3390/ani14010137

Vella, A., & Vella, N. (2023). Conservation Genetics of the Loggerhead Sea Turtle, Caretta caretta, from the Central Mediterranean: An Insight into the Species' Reproductive Behaviour in Maltese Waters. Animals, 14(1), 137. https://doi.org/10.3390/ani14010137

Viola, P., & Jones, M. (2001). Rapid object detection using a boosted cascade of simple features. Proceedings of the 2001 IEEE Computer Society Conference on Computer Vision and Pattern Recognition. CVPR 2001, 1, I-511-I–518. https://doi.org/10.1109/CVPR.2001.990517

Witherington, B., Hirama, S., & Mosier, A. (2011). Sea turtle responses to barriers on their nesting beach. Journal of Experimental Marine Biology and Ecology, 401(1–2), 1–6. https://doi.org/10.1016/j.jembe.2011.03.012

Witt, M. J., Hawkes, L. A., Godfrey, M. H., Godley, B. J., & Broderick, A. C. (2010). Predicting the impacts of climate change on a globally distributed species: The case of the loggerhead turtle. Journal of Experimental Biology, 213(6), 901–911. https://doi.org/10.1242/jeb.038133

World Conservation Union & International Union for Conservation of Nature and Natural Resources (Eds). (1995). A global strategy for the conservation of marine turtles. IUCN.

WWF. (2000). Sea Turtle | Species | WWF. World Wildlife Fund. https://www.worldwildlife.org/species/sea-turtle

Zhao, Z.-Q., Zheng, P., Xu, S.-T., & Wu, X. (2019). Object Detection With Deep Learning: A Review. IEEE Transactions on Neural Networks and Learning Systems, 30(11), 3212–3232. https://doi.org/10.1109/TNNLS.2018.2876865

Zou, Z., Chen, K., Shi, Z., Guo, Y., & Ye, J. (2023). Object Detection in 20 Years: A Survey. Proceedings of the IEEE, 111(3), 257–276. https://doi.org/10.1109/JPROC.2023.3238524